7-5-2018

Design and Implementation of 60 GHz Cavity Backed Patch Antennas

Kasey Chun
Santa Clara University, kkchun@scu.edu

Recommended Citation

SANTA CLARA UNIVERSITY

Department of Electrical Engineering

I HEREBY RECOMMEND THAT THE THESIS PREPARED
UNDER MY SUPERVISION BY

Kasey Chun

ENTITLED

Design and Implementation of 60 GHz Cavity Backed Patch Antennas

BE ACCEPTED IN PARTIAL FULFILLMENT OF THE REQUIREMENTS
FOR THE DEGREE OF

MASTER OF SCIENCE
IN
ELECTRICAL ENGINEERING

Thesis Advisor(s)   6/20/2018
                                                        date

Santa Clara University

Design and Implementation of 60 GHz Cavity Backed Patch Antennas

By: Kasey Chun

A thesis submitted in partial fulfillment for the degree of Master of Science in the Department of Electrical Engineering

Examiner Committee:

Dr. Ramesh Abhari
Thesis Advisor

Dr. Timothy Healy
Thesis Reviewer

Declaration of Authorship

I, Kasey Chun, declare that this thesis titled, 'Design and Implementation of 60 GHz Cavity Backed Patch Antennas' and the work presented in it are my own. I confirm that:

- This work was done wholly while in candidature for a master's degree at Santa Clara University.

- Where any part of this thesis has previously been submitted for a degree or any other qualification at this University or any other institution, this has been clearly stated.

- Where I have consulted the published work of others, this is always clearly attributed.

- Where I have quoted from the work of others, the source is always given. With the exception of such quotations, this thesis is entirely my own work.

- I have acknowledged all main sources of help.

- Where the thesis is based on work done by myself jointly with others, I have made clear exactly what was done by others and what I have contributed myself.

Signed:

Date: 7/5/18

Acknowledgements

I would first of all like to thank my professor, Dr. Ramesh Abhari, for her continued support and motivation throughout the course of the graduate program and my thesis research. I am grateful for everything that she has done for me and I am inspired by her enthusiasm and knowledge. I would not have been able to accomplish what I have without her help.

I would also like to thank my family and friends for always being there for me throughout the years, pushing me to be the best that I can be. They have made me the person I am today and have continued to push me to achieve greatness. I am grateful for all of the experiences and relationships I have built throughout my time at Santa Clara University.

Abstract

As the lower range of radio frequency spectrum become more cluttered and the demand for faster data rates and greater bandwidth grows, next generation wireless technology is pushed to innovate and provide needed resources. Major technology companies such as Samsung, intel, Qualcomm Inc. and Google have been investing at millimeter-wave band frequencies to address this imminent need. The fifth generation of telecommunication technology could be perceived as a paradigm shift in the way we see and think about wireless communication. This next generation technology is intended to enable other up and coming industries and services such as internet of things (IOT), telemedicine and wearable devices. Antennas are the critical component in realizing any of the wireless systems in these emerging applications.

This thesis investigates design and simulation of 60 GHz microstrip patch antennas, in single and array arrangements. A few single patch antennas and 2x2 patch arrays were designed to operate at 60 GHz. The needed feed network for the studied antennas were also developed using microwave design techniques and transmission line theory followed by fullwave simulations to achieve matching at the excitation ports. First, a cavity-backed patch antenna is designed and optimized to maintain and improve the operational characteristics of a single radiating element. Next, via-fence strategy used for implementation of cavity was employed in array design. Extensive fullwave simulations and design trials revealed that at 60GHz, due to comparable dimensions of the microstrip feed network with those of the radiating elements, the overall antenna system radiation performance is impacted.

Hence, a second feed strategy using coaxial probe is utilized for new design iterations of single microstrip patch and 2x2 patch array. For these final designs the feed is via the vertical mount coaxial cable with center pin extended through the antenna substrate. This eliminated the need for a lengthy microstrip transmission line feed and reduced the amount of impedance fluctuations. Cavity backing strategy and via fencing were also included and optimized for these designs to optimize the antenna performance. It was concluded that cavity backing is the most practical approach for antenna system design at 60GHz which was able to improve the front to back lobe ratio of the patch antenna. This feature is very important in applications requiring confinement of radiation in only half space and directing it away from the user such as in health monitoring devices.

Finally, the fabrication process is discussed in detail which involves exporting the design layout from an electromagnetic field solver to another CAD tool to generate fabrication files and define the different components and layers. The connectors and launch pins needed for prototyping have been identified for future fabrication and testing.

Table of Contents

List of Figures

List of Tables

Abbreviations

ADS -- Advanced Design System

BW -- Beam Width

CST -- Computer Simulation Technology

FTBLR -- Front To Back Lobe Ratio

HPBW -- Half Power Beam Width

LTE Long -- Term Evolution

PCB – Printed Circuit Board

SMA -- Surface Mounted Adapter

VNA -- Vector Network Analyzer

VSD -- Vital Sign Detection

Chapter 1 Introduction

1.1 Overview

The long-term evolution (LTE) system of 4G is reaching its limits for supporting the sheer number of devices and data demands in today's network. With 20 billion devices expected to be connected by 2020 and application data continuing to grow at an exponential rate, the next generation of wireless and mobile systems will need a major paradigm shift to support these demands [2]. 5G technology is on the horizon and there are major aspects associated with this shift; an unprecedented number of antennas, high density of devices and base stations and high carrier frequencies which are capable of massive bandwidths.

Much of the lower microwave frequencies have been congested with technologies such as Wi-Fi, Bluetooth, GPS and mobile communications operating at the lower end of the GHz range (below 5GHz). V-Band frequencies, as shown in figure 1.1, on the other hand, have a plethora of untapped bandwidth as the 50 - 75 GHz spectrum has only recently been getting attention within the tech industry. 60 GHz in particular has become a much sought after frequency as a global unlicensed band exists at 57 - 64 GHz. This frequency spectrum has typically been used for military communication but massive technology companies such as Qualcomm Inc. and Google have recently invested in developing nextGen 5G and Wi-Fi at 60 GHz to create a "hyper scalable mmWave networking solution for dense urban [communication]" [1].
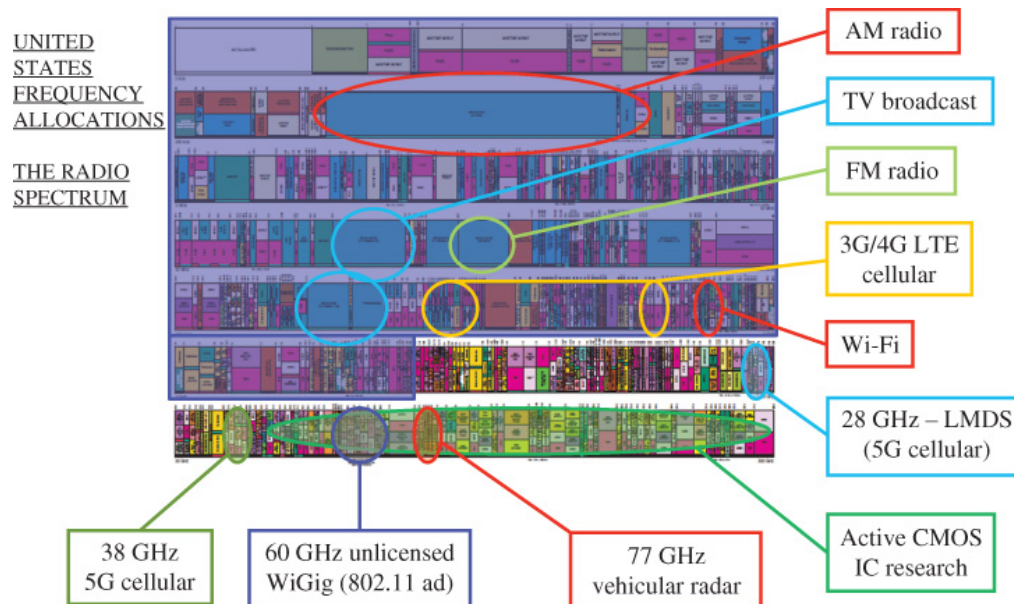
Figure 1.1: Frequency Allocation [20]

Although not fully understood or widely implemented as of yet, the mmWave range has become standardized in the IEEE 802.11ad for short-range services, further demonstrating the growing recognition that this technology is the future of wireless communication. This wireless specification can link devices at up to 7 Gbps over a distance of up to 12 meters, making it 10 times faster than the current 802.11n Wi-Fi technology [1]. Higher frequencies allow for faster data rates but come at a trade-off between lower transmission ranges due to significant attenuation. Oxygen absorption of electromagnetic waves and low material penetration are some drawbacks associated with such high frequency spectrum transmission [5]. Despite these concerns, 60 GHz remains ideal for extra capacity in dense areas/events, ad-hoc networks, cellular backhaul and high speed data links.

Next generation wireless technology also has great potential to be integrated into another growing industry; wearable technology. This term encompasses the integration of electronic devices or processing systems into wearables that include watches, fabrics, spectacles, headbands etc. These devices are often used to relay information to the user or provide more insight about the user themselves. Millimeter waves can provide more accurate information about the user, as the ratio between the wave and vital signs increases, and also supports faster data transmissions for real time updates.

This technology has the potential to change the way we think about and utilize wireless communication. High data rates provided by mmWave technology have many use cases and implications of what is to come in the next generation of RF technology. With up to 7 Gbps of data linkage, we could possibly see a major reduction in the amount of physically wired connections throughout households, businesses and metropolitan areas. Whether implementing more efficient networks or integrating into other technologies such as wearable devices, it is important to create an antenna that maximizes gain and directivity while reducing the amount of backward radiation that wastes power and may cause unwanted effects to circuitry or objects behind the antenna. These far reaching applications and performance considerations serve as the foundational influence for this thesis investigation.

1.2 Thesis Rationale and Objectives

The objective of this thesis is to investigate, design and simulate Microstrip patch antenna designs at 60GHz that are compatible with standard printed circuit board (PCB) technology fabrication process for possible use in wearable devices and other 5G applications. Design of antennas at millimeter wave frequencies dates back to the 1930s and World War 2 when airborne radar frequencies pushed into the K-band and beyond to obtain better angular resolution from apertures limited in size [23]. By the end of the war a "harmonic generator driven by a centimeter-wave

klystron, obtained enough second-harmonic signal to measure the 5-mm wavelength (60Hz)… Thus the period through World War II closed out with the stage set for the extension of coherent radio frequency techniques into the millimeter/submillimeter range" [23].   Disciplinary development of the millimeter-wave spectroscopy progressed and the short wavelength, high power transmission applications supported the use of waveguide to horn antenna topologies. Patch antennas, on the other hand, are easily fabricated and its flat design makes it ideal for use in wireless technology and wearable devices. Figure 1.2 below shows an example of a horn antenna compared to a ring of patch antennas (which are being utilized on a Cisco access point for precise location detection of wireless devices).
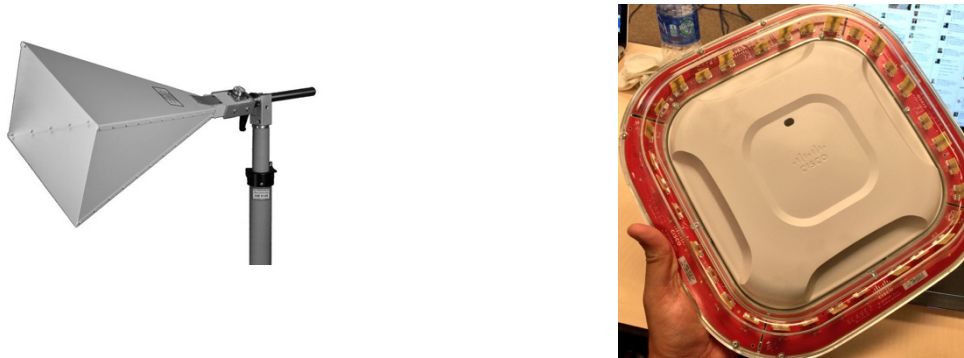
Figure 1.2: Horn vs Patch Antenna [21][22]

Microstrip patch antennas, shown in figure 1.3, were first officially introduced in the IEEE Transactions on Antennas and Propagation in 1974 [24]. In a way they were a breakthrough in development of electronic systems since they provided a low profile antenna that can be fabricated using PCB fabrication technology. Ideally, there is an infinite conductor (ground) plane at the back of microstrip patch antenna to direct antenna radiation towards the upper half space above the microstrip patch. In practice this is not possible and a finite size ground plane is used which results in radiation lobes (known as back lobes) towards the lower half space below the ground plane.
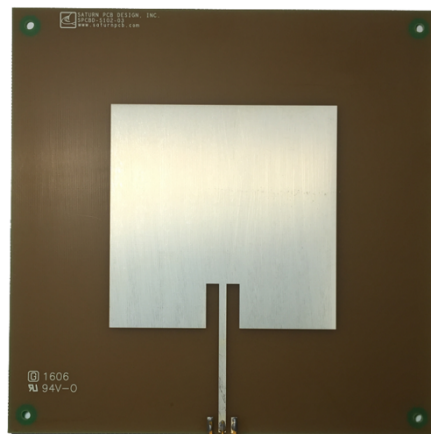
Figure 1.3: Patch Antenna [25]

Waveguide based antennas such as the horn antenna shown in figure 1.2 and cavity backed antennas are among those antenna topologies that provide minimal radiating back lobes. Cavity backed microstrip antennas exhibit superior performance due to their salient features of surface wave suppression, isolation from the surrounding, reduced coupling and better matching [27]. Modern PCB fabrication technology has enabled easy integration of waveguide and cavities in printed circuit boards systems by using via fence structures. Therefore, in this thesis, after investigating the design and simulation of single microstrip patch antenna, a cavity backed microstrip patch antenna is studied and designed for operation at 60GHz.

Since at mm-wave frequencies the dimensions of the antennas are on the order of few mm, in order to increase radiation gain often an array of the same radiating elements is used. In addition to increasing the gain, antenna arrays offer capabilities such as pattern shaping, beam scanning and switching. The arrangement of antennas in an array could be along a line or plane. The former is known as linear array and the latter as planar array. After studying a single patch element at 60mGHz, a 2 by 2 planar patch antenna array is investigated in this thesis.

Ultimately the design of a 2x2 patch antenna with cavity backing and operating at 60 GHz is the intended goal for this thesis. Based on the conducted literature survey it is expected that the 2x2 antenna array increases the gain and bandwidth of the electromagnetic radiation, and the cavity backing provides further directivity and bandwidth improvement as well as reducing backward radiation. One other important feature that results from using the cavity backing method is the reduction of unwanted interference and substrate noise generated by other devices and/or circuitry sharing the same substrate as the antenna. 60 GHz wave transmission traditionally results in a narrow beam width and high attenuation, so creating a passive design to increase font to back lobe ratio, bandwidth and directivity to mitigate the natural deficiencies of transmission is the ultimate goal.

The procedure for going about creating a final design first requires designing the patch antenna using the available analytical formulas, followed by simulation and analysis of a single patch antenna, with and without a cavity using fullwave electromagnetic field solvers. Advanced Design System (ADS) and Computer Simulated Technology (CST) are two software simulators that are utilized throughout this thesis. ADS is typically used for circuit simulations with active components but can also be used for planar antennas and is based upon Method of Moment for calculations and analysis [26]. CST on the other hand is a 3-D EM simulator based on Finite Integration in Technique for computing radiation patterns and antenna performance and is widely popular for antenna design [26]. Both ADS and CST were used to evaluate the performance of designed patch antennas with different cavity designs. From there the basic design layout is expanded to a 2x2 structure with the proper design of the antenna array feed network. The design of the microstrip feed network is based on a series of quarter wave microstrip transmission lines that are intended to create a path from input to patch with as little loss as possible. In addition, the effects of a microstrip fed design was compared to a probe-fed design. The probe-fed design was found to be a more practical and effective way of feeding the patch antenna.

As the project moved forward, material restrictions required the need to move from a Duroid 5880 substrate to a R05340 substrate. This provided an opportunity to compare results of different substrates and examine the effects the substrate on cavity design considerations and the resulting performance of the cavity backed patch antenna.

1.3 Thesis Outline

The thesis has been organized as follows:
Chapter 2 discusses the designed background of patch antennas. This includes single patch physics, feed techniques and cavity backing research. Chapter 3 describes evaluation of a 2x2 patch array at 60 GHz and its comparison with a designed model. In addition a solid cavity backing instead of using via fence walls is investigated in this chapter. Chapter 4 takes this design technique and applies it to a new R04350 dielectric material. Again a single patch and a 2x2 patch array are investigated using this substrate, and the backing cavity is designed. In Chapter 5 a probe fed patch is designed and extended to an array implementation. For this new set of 60 GHz probe-fed antennas, new cavity backing structures should be designed by optimizing the via fence walls as also discussed in Chapter 5. Chapter 6 discusses a sample application of a remote vital sign detection at 60 GHz using patch antennas. The higher frequency can offer much more accurate health information than lower frequency antennas and a cavity backed patch is ideal for wearable devices and can be optimized to achieve more desirable antenna characteristics. Chapter 7 details all the steps needed for fabrication of four chosen designs of single and 2x2 patch array antennas for future prototyping and measurement. The concluding remarks for the entire thesis, including future work suggestions are detailed in Chapter 8.

Chapter 2 Microstrip Patch Antennas

Microstrip patch antennas are very widely used designs throughout the technology industry. The low cost, low profile and ease of fabrication makes patch antennas ideal for a number of mobile device applications [2]. Microstrip patch antennas can be printed directly onto circuit boards and the design procedures for known substrate characteristics are well documented, with closed formulas used for layout dimension calculations.

2.1 Designs and Calculations for Patch Antennas

A basic patch antenna consists of a conductive microstrip land printed on a dielectric substrate that is covered with a solid conductor ground plane on the other side (See figure 2.1). The patch antenna can be fed using multiple techniques but the most common are a microstrip line or a coaxial probe feed, both of which are shown in figure 2.1 below. These feeding techniques will be discussed further, in Section 2.2.
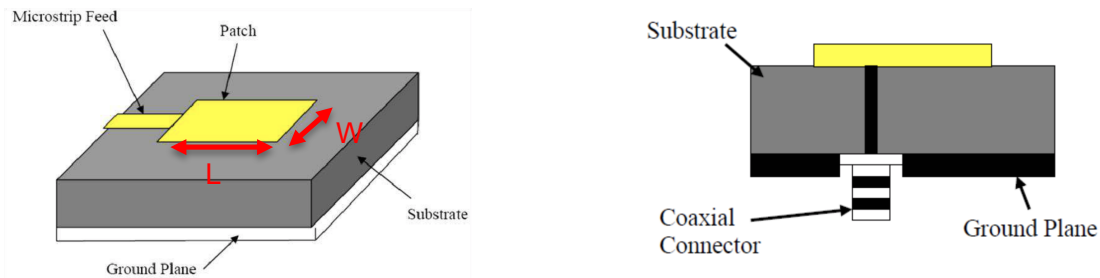
Figure 2.1: Basic Patch Antenna [3][4]

The shape of the patch can be anything from square, rectangular, circular, elliptical or any combination but for the purpose of this thesis a rectangular shape is utilized for its well documented nature.

In designing the dimensions of the patch antenna it is essential to know some characteristics of the dielectric being utilized. First is the relative permittivity, εr, of the substrate. This is also referred to as the dielectric constant of a substrate. The second characteristic that is taken into consideration when designing the patch is the height of the dielectric. In general, a thick substrate with low permittivity is desired as thin, high permittivity results in a reduction in antenna size at the cost of gain and matching bandwidth of the signal due to increased losses within the substrate

[5]. It should be noted, however, that the thickness should be limited to avoid excitation of surface waves which degrade radiation efficiency especially at mm-wave frequencies.

The final factor in calculating the dimensions of the patch is the desired resonance frequency. As current flows, the patch can be seen as a transmission line with the ends being open circuits. This results in a reflection coefficient of 1 and, as can be seen in figure 2.2, the voltage at one end is maximized and minimized at the other end. This also results in current being zero at each end and maximized in the center of the patch. As these fields fluctuate back and forth, electromagnetic waves are created and propagate outward.
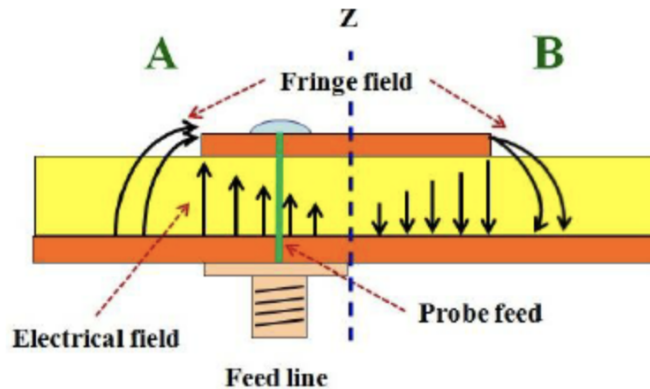
To determine the width (W) and length (L) of the patch we can use available well-known closed-form formulas. Due to the resonating characteristic of the patch antenna as described above, the L of the antenna can be approximated to be half of the wavelength of the desired frequency, however fringing effects on the side of the antenna require an adjustment in the equation as shown in the following equation:

Equation 2.1

$$L = Leff - \Delta L$$

Where the effective length is defined by:

Equation 2.2   *Figure 2.2: Patch Antenna Resonance [6]*

$$Leff = \frac{c}{(2 \cdot f \cdot \sqrt{\varepsilon eff})}$$

And the length extension is defined by:

Equation 2.3

$$\Delta L = 0.412h \frac{(\varepsilon eff + 0.3)(W/h + 0.264)}{(\varepsilon eff - 0.258)(W/h + 0.8)}$$

The effective dielectric constant is found from the formula:

Equation 2.4

$$\varepsilon eff = \frac{\varepsilon r + 1}{2} + \frac{\varepsilon r - 1}{2}[1 + 12W/h]^{-1/2}$$

If c is the speed of light, f is the resonant frequency, and h is the thickness of the dielectric, the width is defined by:

Equation 2.5

$$W = \frac{c}{2f\sqrt{\frac{\varepsilon r + 1}{2}}}$$

This is the initial way of determining the layout parameters for any single patch antenna. Often tweaks and adjustments need to be made to optimize the patch but these formulas serve as the base for initial design. The feed for these antennas can vary, as will be discussed in section 2.2, but the main consideration for the feed is to have the point of contact between the feed and the antenna be of equal impedance (when the antenna input impedance is purely real) to decrease the amount of signal reflection back to the feed.

Single antennas can be expanded to an array of antennas utilizing multiple different techniques. In general, for equally excited linear arrays to have a maximum radiation in the broadside direction the center to center spacing between the patches should be close to a free space wavelength (seen as a half wave length edge to edge spacing) but design area constraints often see this configuration altered. Figure 2.3 shows a few designs for patch antenna arrays with microstrip feed lines.
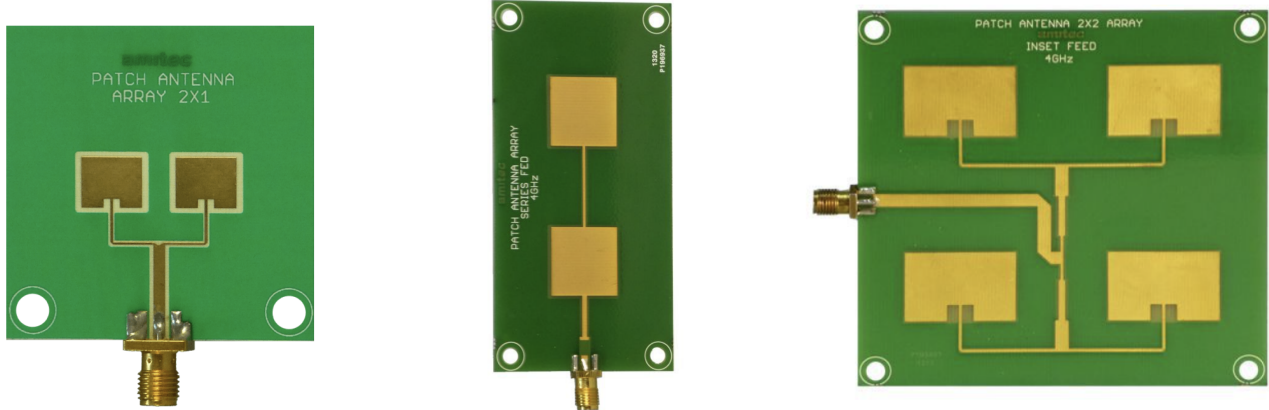
Figure 2.3: Patch Antenna Array with corporate feed (left and right boards) and series fed design (middle) [7]

The theory of antenna array design offers a wide range of mathematical models, design strategies and feed arrangements which are not within the scope of discussion here. Array elements can be phased and excited according to different mathematical polynomials to create high gain arrays or phased arrays for beam steering. The fact that these radiation parameters can be controlled with electronic switches, amplifiers and phase shifters and even with passive delay elements, such as transmission line delay lines, makes this a widely researched field.

2.2 Antenna Feed Types

Section 2.1 discussed the design considerations and procedures for creating the patch antenna itself, but this antenna still needs some source of current to enable electromagnetic radiation. This is where antenna feed comes into play. The main purpose of a feed is to provide a path for electrons to flow into the antenna with as little impedance mismatch as possible. There are many different ways to feed an antenna but two of the most common methods for patch antennas are through the use of a microstrip transmission line or a probe fed through pin. Both methods need to be designed correctly to match the 50 Ω cable, often a coaxial cable, to the point of contact with the patch antenna.

2.2.1 Microstrip Transmission Line Feed

The microstrip transmission line is probably the most basic and widely used way of feeding a patch antenna. This feed can easily be printed onto the circuit board in the same way the patch antenna is and there are well established formulas to design the feed. The point of contact with the patch is often centered at the edge of the width of the patch as shown in figure 2.4 below.
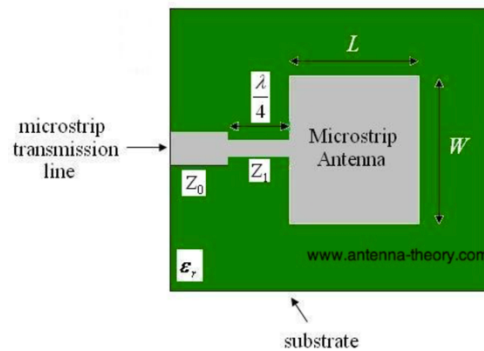
Figure 2.4: Microstrip Transmission Line Fed Patch Antenna [12]

The impedance at the desired point can be derived from the given formula:

Equation 2.6

$$Za = 90(\frac{\varepsilon r^2}{\varepsilon r - 1})(L/W)^2$$

Knowing that you have an impedance of Za at one end of the transmission line and an impedance of 50 Ω at the other end, we can use a closed-form formula to calculate the desired characteristic impedance of the transmission line. The general formula for calculating the input impedance of a transmission lined terminated to a load with the impedance Zl is shown below. From this formula the needed characteristic impedance for transmission line can be calculated.

Equation 2.7

$$Zin = Zo[\frac{Zl + jZo(\tan(\beta L))}{Zo + jZl(\tan(\beta L))}]$$

Where $\beta = 2\pi/\lambda$ and Zl is the load impedance (Za from the previous equation), Zin is the input impedance (usually 50 Ω) and Zo is the characteristic impedance of the transmission line. By creating a quarter wavelength transmission line we can substitute L for $\lambda/4$ thus simplifying the equation to:

Equation 2.8

$$Zin\left(L = \frac{\lambda}{4}\right) = \frac{Zo^2}{Zl}$$

$$Zo = \sqrt{ZinZl}$$

This characteristic impedance can then be used to design the dimensions of the transmission line. Further quarter wavelength segments can be utilized to extend the feed and increase the bandwidth or alter the design of the patch antenna and change W.

Having an input impedance that deviates greatly from the 50 Ω impedance is not ideal, therefore other techniques known as inset feed are used which is shown in figure 2.5. The inset feed design parameters are R, depth of feed penetration in the patch and the gap spacing between the feed and the patch. The impedance at the point of contact of the inset feed with the patch is closer to 50 Ω and can be controlled with selection of R.
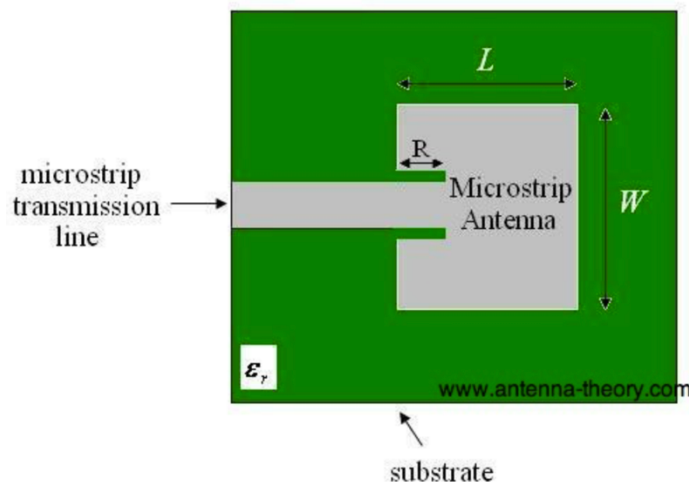
Figure 2.5: Inset Feed Microstrip Transmission Line Feed [12]

This point of contact impedance of the patch as a function of R in the inset feed can be calculated from the formula below [12]:

$$Zin(R) = \ cos^4\left(\frac{\pi R}{L}\right)Zin(0)$$

Depending on the desired complexity and need for impedance matching, any one of these microstrip transmission line techniques are viable feed solutions.

2.2.2 Probe Through Pin Feed

The other method for feeding a patch antenna utilizes a through pin to connect the source to the antenna. This involves a vertical mount surface mounted adapter (SMA) placed on the ground plane. The center conductor of the SMA (referred to as probe herein) penetrates through the dielectric and connects to the patch antenna, allowing current to flow from the source, through the coaxial cable, up to the probe and onto the patch. This design is shown in figure 2.6 below.
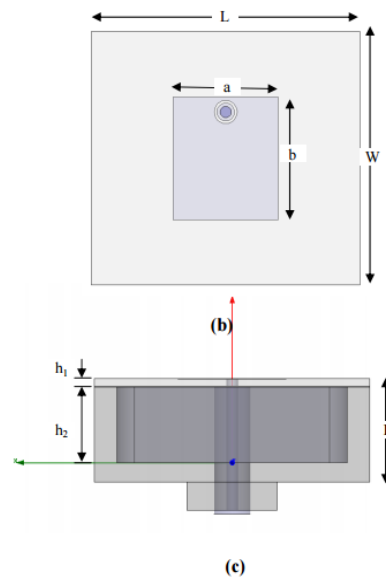
Figure 2.6: Probe Fed Patch Antenna [9]

Similar to the inset microstrip feed, at the point where the probe pin meets the patch impedance match should be achieved to reduce reflection. To find the point where the probe should contact the patch antenna we can also use a similar formula as the microstrip transmission line feed except for the fact that the power of cosine function is 2 instead of 4.

As you can see, there are multiple different ways to feed a patch antenna. Deciding on which method to choose may come down to design constraints or desired results, but the main thing to keep in mind is ensuring that the current from input cable with an impedance of 50 Ω reaches the patch itself with as little loss and/or reflection as possible. For this reason, a probe fed antenna is often more efficient especially at mm-wave frequencies as it reduces the amount of losses and possible mismatches due to transmission line propagation and radiation but both methods are effective and widely used.

2.3 Cavity Backed Patch Antenna

Microstrip patch antennas have their benefits, including low profile, light weight and ease of fabrication as discussed in previous sections, but they also have their drawbacks. Issues with surface wave propagation which is inherent in patch antennas cause a reduction in the efficiency and gain, and limit the bandwidth and frequency range of the antenna [10]. There is also significant backwards radiation that reduce the directivity of the patch antenna and may have harmful effects on other components or materials that may lie behind the antenna itself. A cavity backed patch antenna aims to reduce these adverse effects by creating a container, or cavity of sorts, to reduce the amount of wasted power due to surface wave propagation and back radiation. This cavity can either be composed of 4 metallic walls that cover the four sides of the antenna or of a multitude of metallic via holes that encompass the antenna [10].

The design of the cavity has a great effect on the resonance, radiation and power efficiency of the patch antenna. In general, this encasing should be about 2 times the length of the patch antenna, as shown in figure 2.7 where R = 2a [11]. After a simulation of varying distances for the cavity width the survey in [11] ultimately concluded that an R of 1.8a is ideal for rectangular patches with a rectangular cavity.
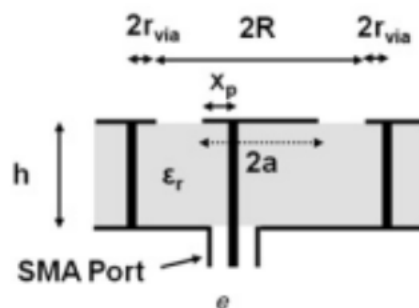
Figure 2.7: General Cavity Design [11]

Designing the via hole sizes and spacing can also have drastic effects on the performance the patch antenna. D and S shown in figure 2.7 represent the diameter of the vias and the spacing between them, respectively.
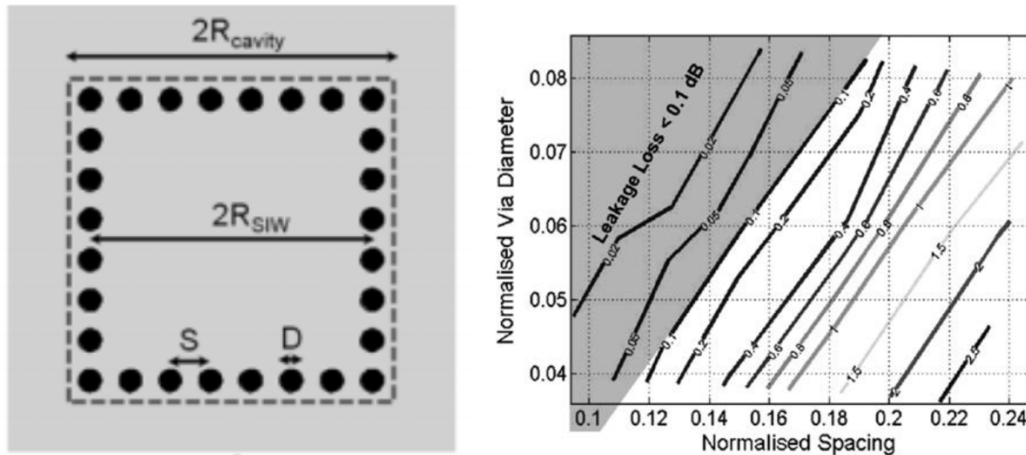
Figure 2.8: General Via Cavity Design and reported Simulation Results from [11]

Fullwave parametric simulations have been conducted while changing S and D variables at the design frequency of 2.4 GHz in [11] with the results shown in figure 2.8 Ranging S from 0.1mm to 0.25mm and D from 0.04mm to 0.09mm resulted in the optimized dimensions of S = 0.14λ and D = 0.059λ.

These design considerations and surveyed results served as the base line for creating the cavity backed patch antenna that is discussed in the rest of this thesis.

2.4 Conclusion

This chapter discussed how a microstrip patch antenna works and how to design one using closed formula equations. Different feed methods are also introduced, comparing microstrip and probe feed lines and showing ways to design them. Finally cavity backed designs are investigated and a reference article [11] is used as the base for further research. These designed and surveyed models for creating patch antennas are utilized and tweaked throughout the rest of this thesis. The design strategies follow all of the different methods discussed in this chapter, moving from a microstrip single patch, to a microstrip patch array and then creating a cavity backing for the antennas. The equations and surveyed results in this chapter serve as a reference for the subsequent chapters.

Chapter 3 Antenna Design At 60 GHz On Duroid 5880

This chapter will discuss the process of designing and simulating a patch antenna array optimized at 60 GHz utilizing the Duroid 5880 substrate. The original survey presented in [8] was used as the foundation for initial designs and simulations. This report used a Duroid 5880 substrate with a dielectric constant of 2.20 and a height of .127 mm to create a 2x2 patch antenna array operating at 60 GHz. This design is first validated and analyzed, then built upon to include a cavity backing.

3.1 Single Patch Antenna Design and Simulation

This section will discuss the process of designing and simulating a single patch antenna optimized at 60 GHz. Using the survey from [8] as a sample, the first step involves analyzing just a single patch then developing a theoretical patch with a microstrip transmission line feed and finally designing a cavity backing for the single patch.

3.1.1 Surveyed Single Patch Antenna Analysis

The original design and result of the 2x2 patch antenna on a Duroid 5880 substrate is shown in figure 3.1 with the results shown in Figure 3.2. However, before diving into this multi-patch array the characteristics of a single patch should be analyzed.
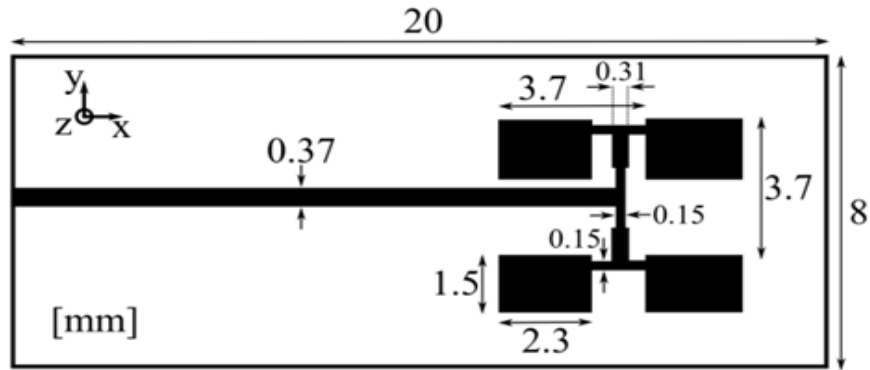
Figure 3.1: 2x2 Surveyed Patch Array [8]
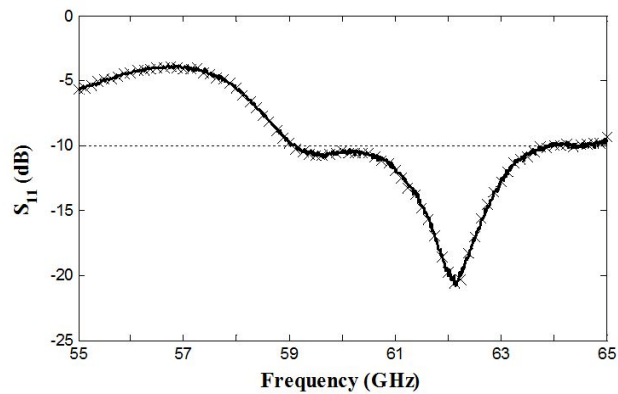
Figure 3.2: 2x2 Surveyed Patch Array Results [8]

According to this document, a single patch is 2.3 mm in length and 1.5 mm in width with a feed input located around 1 mm from the edge of the patch. This patch is recreated in ADS, shown in figure 3.3, and the results are shown in figure 3.4.
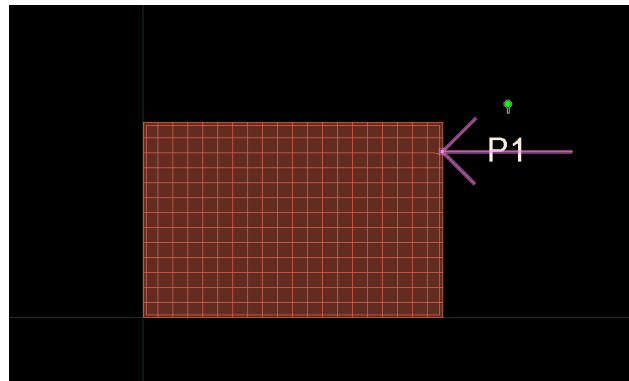
Figure 3.3: Surveyed Single Patch in ADS
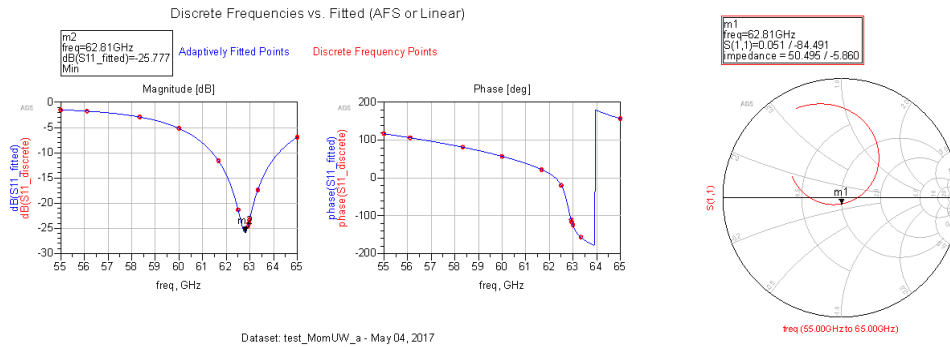
Figure 3.4: Surveyed Single Patch in ADS Results

From these results it can be seen that the input impedance is 50.5 Ω and the patch resonates at 62.81 GHz with an S11 value of -25.777 dB. The resonance frequency from [8] seen in Fig. 3.2 is 62.1 GHz with S11 of -21.8 dB. ADS is a 2.5D field solver which uses method of moment for electromagnetic field solution. For a more accurate simulation after adding a 50 Ω transmission line a 3D fullwave solver CST simulation is used for simulations to see how the results compare. This design is shown in figure 3.5 with the results shown in figure 3.6.
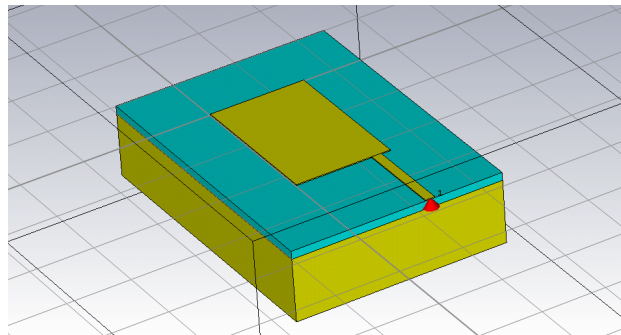
Figure 3.5: Surveyed Single Patch in CST
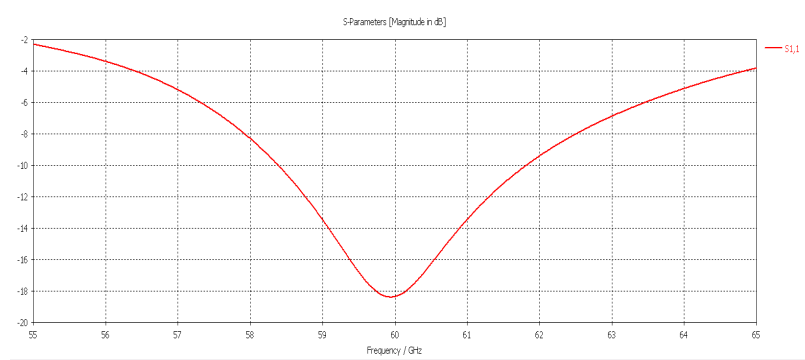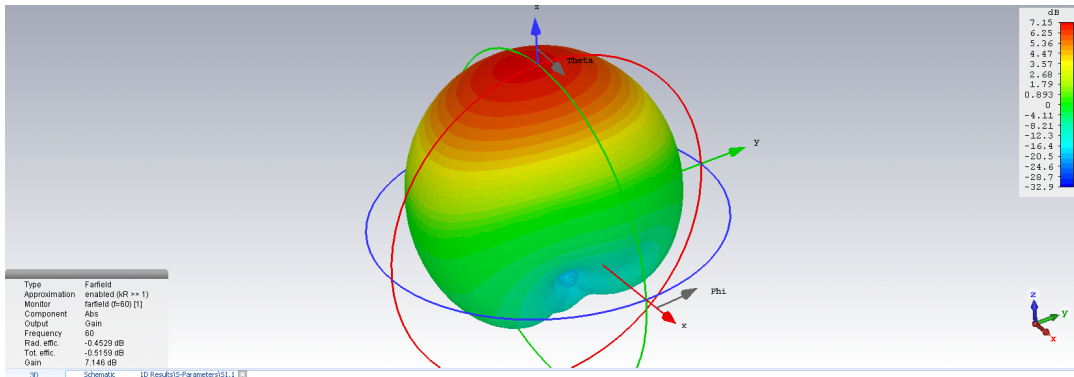
Figure 3.6: Surveyed Single Patch in CST Results

From this CST simulation we can see that the patch resonates right at 60 GHz with an S11 of -18.5 dB. The directivity and gain are 7.5999 dBi and 7.146 dB respectively with an efficiency of 88.8%. Although survey [8] did not explicitly measure a single patch antenna component, this gives us an idea of what a single patch operation looks like compared to a patch array, which is designed out in further sections.

This single patch seems to operate well at 60 GHz but there is no guarantee that the performance stays the same in an array arrangement especially at mm-wave frequencies and the design has to be optimized for a 2x2 patch array.

In the next section theoretical design of a single patch antenna with a transmission line feed is presented to see how the added feed lines impact the antenna performance.

3.1.2 Designed Single Patch Antenna Analysis

Using the formulas discussed in section 2 we can create a patch antenna optimized at 60 GHz with a width 1.97 mm and a length of 1.62 mm. For brevity the so designed patch is called "theoretical patch antenna" or "designed patch antenna". Nonetheless, the layout determined according to theoretical formulas is created in ADS layout window for fullwave simulation. A quarter wavelength transmission line feed is designed with a width of 0.1 mm and a length of 0.94 mm to match the calculated input impedance of the antenna at the edge (ZA = 144 Ω) to a 50 Ω microstrip feed. From ADS microstrip calculator or microstrip line design formulas the width of the 50Ω line was calculated to be 0.35mm. The length of this line was considered 3.64 mm. The layout of this design can be seen in figure 3.7 with the S11 and VSWR plots presented in figure 3.8.
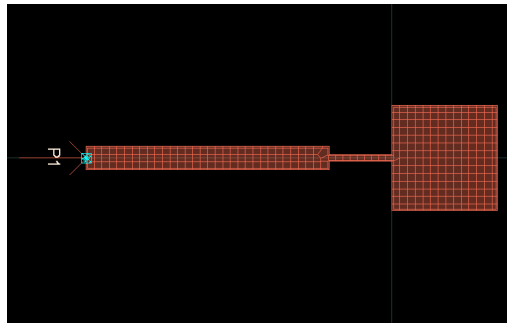
Figure 3.7: Designed Single Patch in ADS

Dataset: cell_1_MomUW_a - Apr 20, 2017
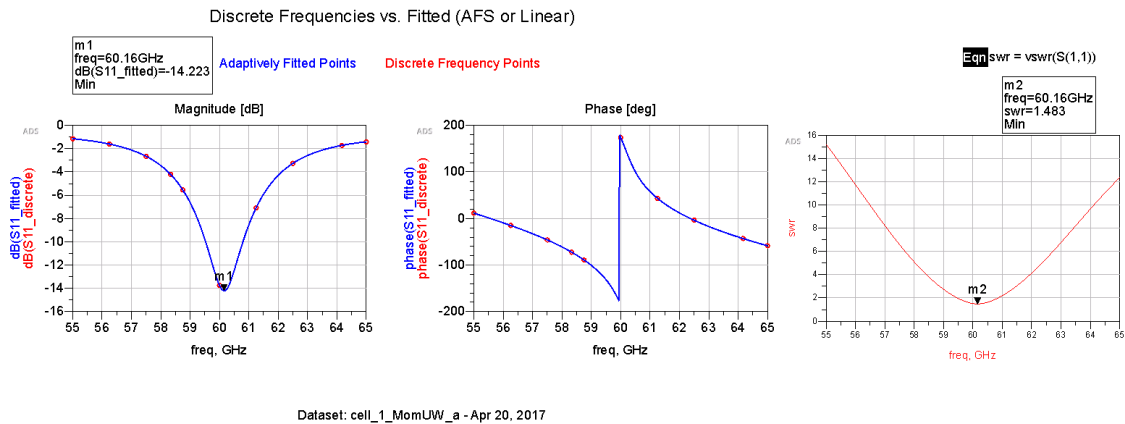
Figure 3.8: Designed Single Patch in ADS Results

The ADS results show that the patch resonates right at 60.16 GHz with an S11 of -14.223 dB and VSWR of 1.483. This theoretical design seems to match the desired 60 GHz operational frequency perfectly but in order to compare it side by side with the surveyed microstrip fed patch antenna from section 3.1.1, it is beneficial to recreate the layout in a 3D fullwave solver such as CST to ensure similar condition in simulations. The CST design can be seen in figure 3.9 with the results in figure 3.10.
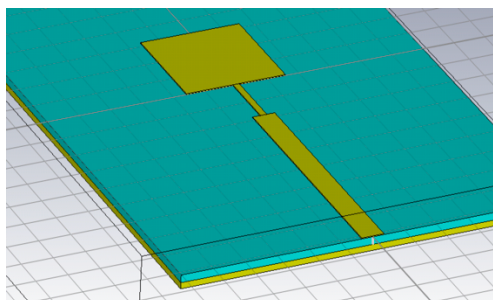
Figure 3.9: Single Patch in CST
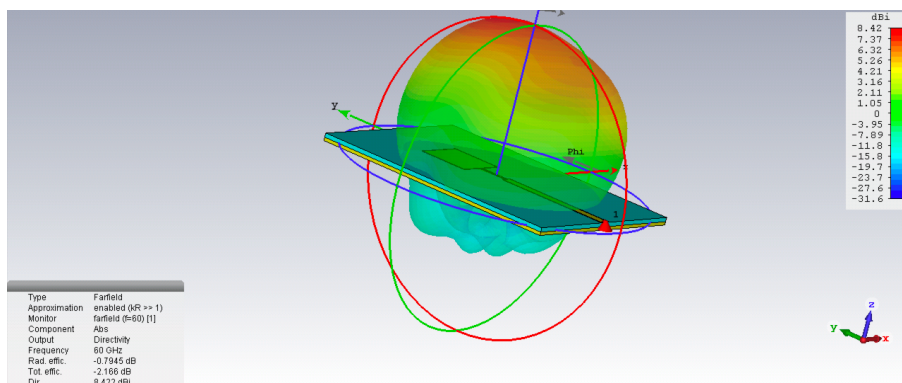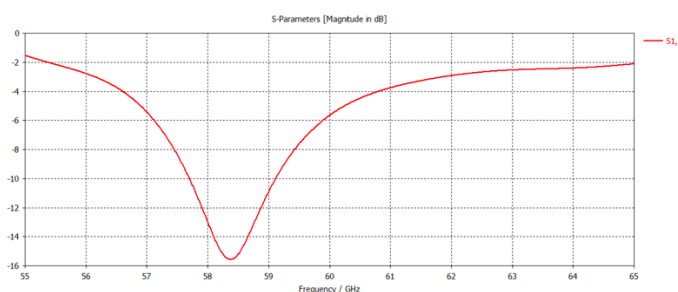
Figure 3.10: Designed Patch in CST Results

The CST simulation results show the patch resonates at 58.39 GHz with an S11 of -15.56 dB. One of the major factors that contributes to the different results in ADS versus CST is the fact that ADS simulates the layout assuming an infinite ground plane while CST assumes a finite size backing ground plane.

The simulated gain and directivity from CST are 7.627 dB and 8.422 dBi respectively and an efficiency of 77.93% is achieved. In both scenarios, the ADS simulation resulted in a slightly higher resonant frequency with less reflection, however CST is more accurate when simulating 3D EM radiation which is why we see more losses and a more realistic result. The theoretical design actually results in a less ideal performance when simulated in CST compared to the

surveyed antenna in section 3.1.1. The comparison is shown below in table 3.1, but it is clear that the surveyed design has been optimized for 60 GHz.

Property	Surveyed Antenna	Designed
Resonant Frequency	60 GHz	58.39 GHz
S11	-18.5 dB	-15.56 dB
Gain	7.146 dB	7.627 dB
Directivity	7.5999 dBi	8.422 dBi
Efficiency	88.8%	77.93%

Table 3.1: Single Patch Surveyed vs Designed

3.2 Patch Array Design and Simulation

After investigating the single patch antenna the next step involves researching an antenna array. To achieve the final 2x2 design, a 2x1 patch array is created first, utilizing the single patch design developed in Section 3.1. The 2x1 patch is then extended to a finalized 2x2 patch array. As in the previous section, the surveyed design is created and validated, then compared to a theoretically designed model.

3.2.1 Surveyed Patch Array Analysis

From the surveyed design the 2x1 patch array is fed by a transmission line with a width of 0.31 mm and a length of 0.95 mm ("a" in figure 3.11) which splits into 0.15 x 0.7mm feeds into the 2 patches ("b" in figure 3.11).

Figure 3.11: Simulated layout of the Surveyed 2x1 Patch in ADS
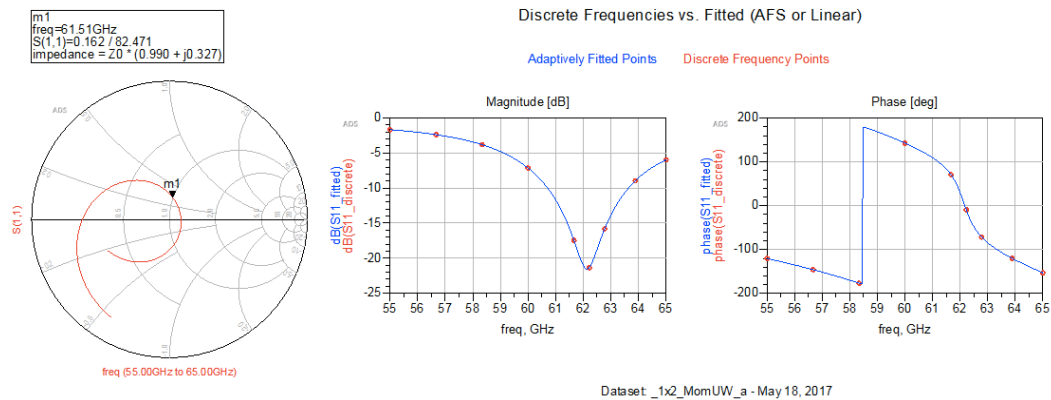
Figure 3.12: Simulations of the Surveyed 2x1 Patch in ADS Results

The results presented in figure 3.12 show that the input impedance of the 2x1 antenna is 52.1 Ω . Feed "a" which is a quarter-wave transformer has a characteristic impedance of 57.99 Ω . This means the impedance seen at the beginning of the T junction should be 64.54 Ω (*Zl*) for matching to *Zin*=50Ω at the other end of the quarter-wave transformer according to the $Zo = \sqrt{ZinZl}$ formula.

Now let's focus on section labeled as Feed "b" that creates two arms of the T junction. Feed "b" has a width of 0.137 mm which yields a characteristic impedance of 86.59 Ω from microstrip characteristic impedance calculation formulas. Knowing that the input impedance of the patch is 50.5 Ω , from section 3.1.1, the calculations for Feed "b" which is another quarter wave transformer results in an impedance of 148.47 Ω at the T junction' start of the Feed "b" transmission line. At the T junction, there are two Feed "b" lines that are in parallel, therefore the equivalent resistance at the T looking toward the two arms is simply half of 148.47 Ω which is 74.24 Ω . This does not perfectly match the 64.54 Ω calculated in the previous paragraph for Feed "a" and labeled as *Zl* (the impedance where this junction intersects with Feed "a". Nonetheless, the simulations show an S11 of -21.5 dB at the input of Feed "a" which is a decent match for this patch antenna. The results also show that the patch resonates at 62 GHz which is higher than we would have expected. Therefore, the reason for slight deviation from calculated *Zl* 64.54 Ω should be that the patch antenna input impedance is not exactly 50.5 Ω and is higher.

From the analysis 2x1 linear sub-array, we can build the final 2x2 planar patch array. The transmission line feeding into the 2x1 patch array (labeled "c" in figure 3.13) has a width of 0.15 mm and a length of 1.649 mm and the transmission line that connects to the 50 Ω input port (labeled "d" in figure 3.13) has a width of 0.37mm and a length of 15mm.
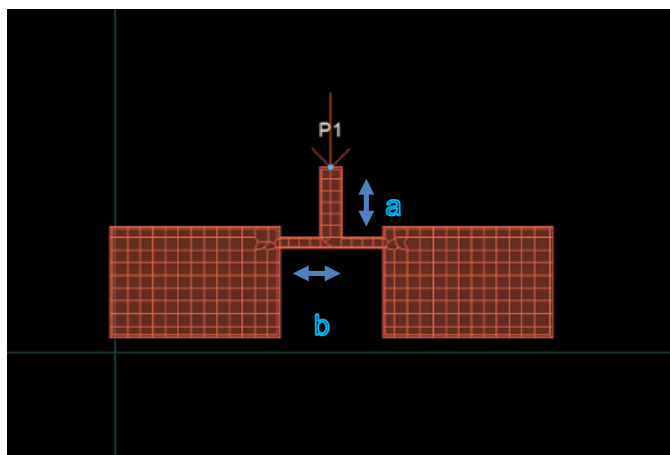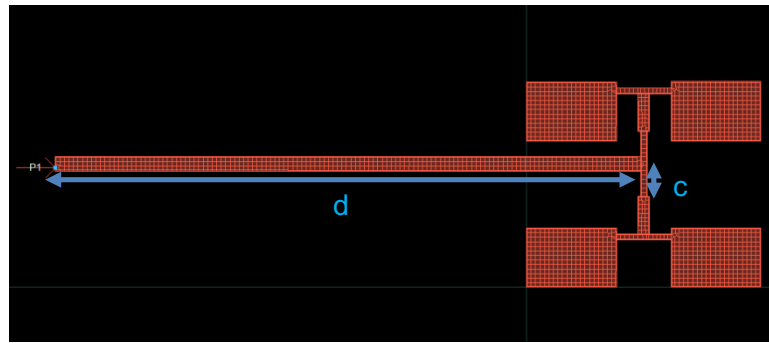
Figure 3.13: Simulated layout of the Surveyed 2x2 Patch in ADS
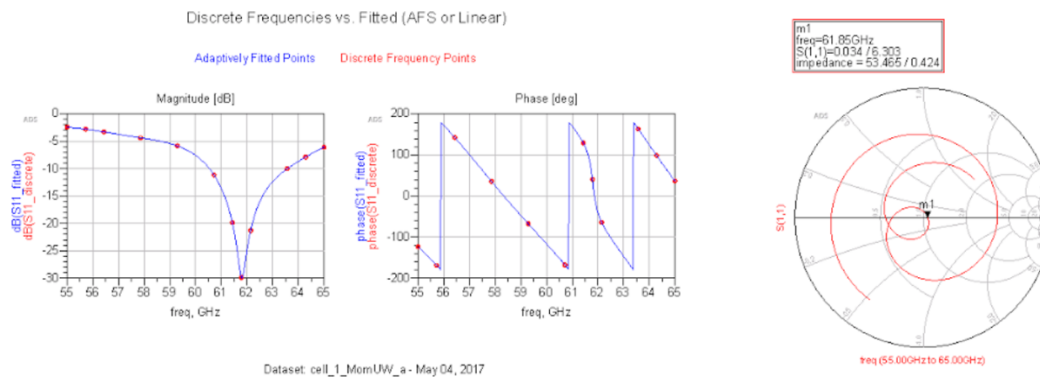
Figure 3.14: Simulations of the Surveyed 2x2 Patch in ADS Results

From the Smith chart shown in figure 3.14 it can be seen that the input of the entire 2x2 patch array has an impedance of 53.46 Ω at the resonance frequency, matching closely to the desired 50 Ω input. Using characteristic impedance formulas indicates that the transmission line "d" has a characteristic impedance of 51.8 Ω . Using the standard formula for calculation of the input impedance of a transmission line yields an impedance of 50.19 Ω at the end of the transmission line (junctions of c and d lines). The characteristic impedance of transmission line "c" is calculated to be 86.6 Ω . At the junction where line "c" meets line "d" a parallel connection exists. For each branch the 86.6Ω line "c" transfers the impedance that is simulated to the junction using the quarter-wave-long line "c" and the ultimate parallel impedance of 43.3 Ω at the junction is calculated. This seems like quite a drastic mismatch, and we see that the patch seems to resonate at 61.6 GHz with an S11 value of -30 dB, and an S11 of -13.5 dB at 60 GHz is observed.

To further investigate mismatch and the S11 behavior and get a more accurate idea of the antenna characteristics, the layout is constructed in CST as shown in figure 3.15 and the radiation characteristic plots are depicted in figure 3.16.
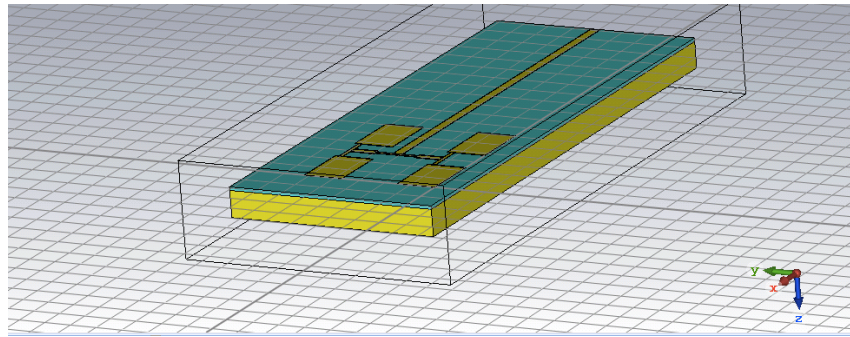
Figure 3.15: Simulated layout of the Surveyed 2x2 Patch in CST
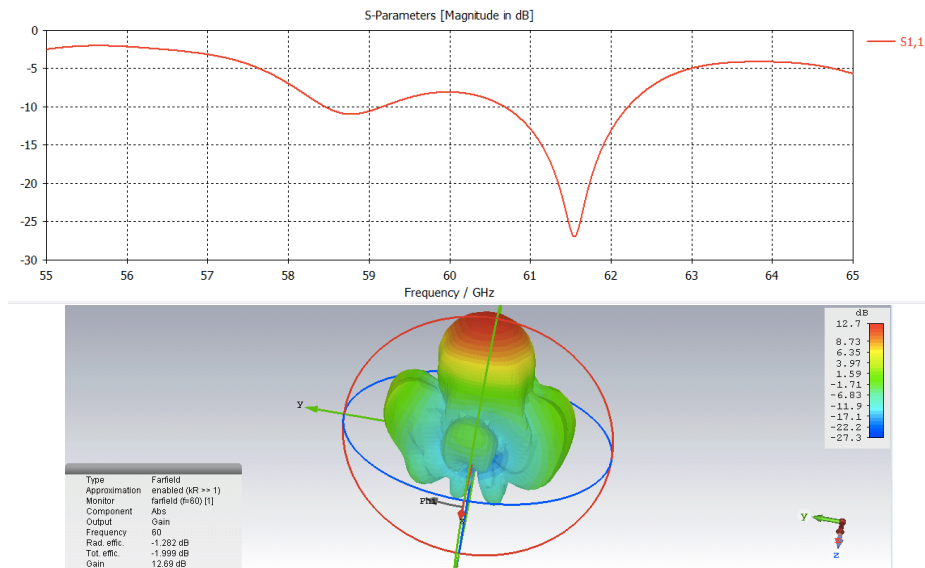
Figure 3.16: Simulations of the Surveyed 2x2 Patch in CST

These results are quite different from ADS simulation results. The S11 bandwidth has increased from the single patch and the pattern closely resembles the documented result from section 3.1.1. This re-creation validates the surveyed document and design.

3.2.2 Designed Patch Array Analysis

A second iteration patch antenna array is designed using theoretical formulas to operate at 60 GHz. Building off of the single patch in section 3.1.2, a 2x1 and then a 2x2 patch array is built and compared to the surveyed antenna in the previous section. In creating the 2x1 patch antenna,

the quarter wave transmission line posed some immediate issues. When being fed to the center of the 2 patches, the transmission line feed would not clear the patches themselves, which would cause problems down the line when 2 more patches would eventually be connected. To get around this, the feed is moved slightly towards the edge of the patch, while maintaining the 50 Ω impedance at that point. With this design the transmission line feeds effectively clear the patches and allow space for further connections to another patch array.

The 2x1 patch design in shown in figure 3.17. The 50 Ω input impedance of the single patch is fed by a quarter wave transmission line which will terminate to 100 Ω ("b" in figure 3.17). This results in a desired characteristic impedance of 70.1 Ω and dimensions of 0.213 mm x 0.931 mm. The parallel antennas result in an impedance of 50 Ω at the junction, so a 50 Ω quarter wave transmission line is used to feed this junction ("a" in figure 3.17). The 50 Ω transmission line is 0.37 mm x 0.912 mm. This should give an impedance of 50 Ω at the P1 input.
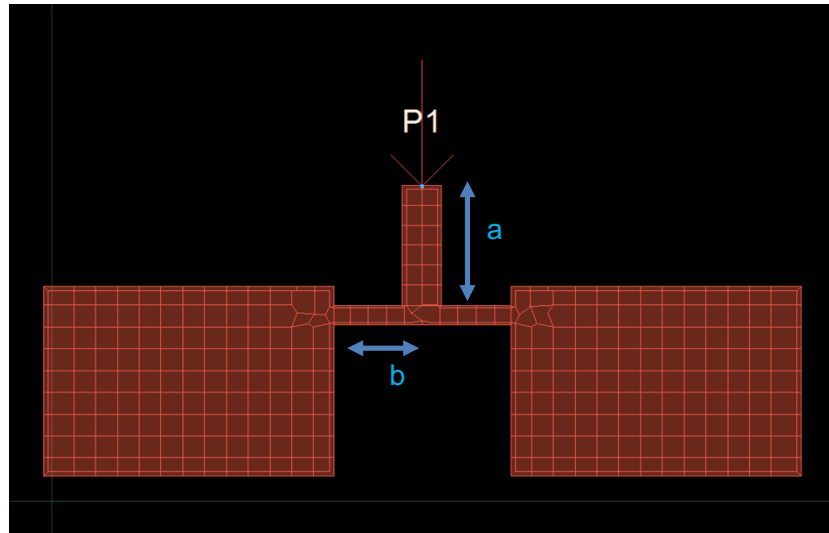
Figure 3.17: Designed 2x1 Patch in AD
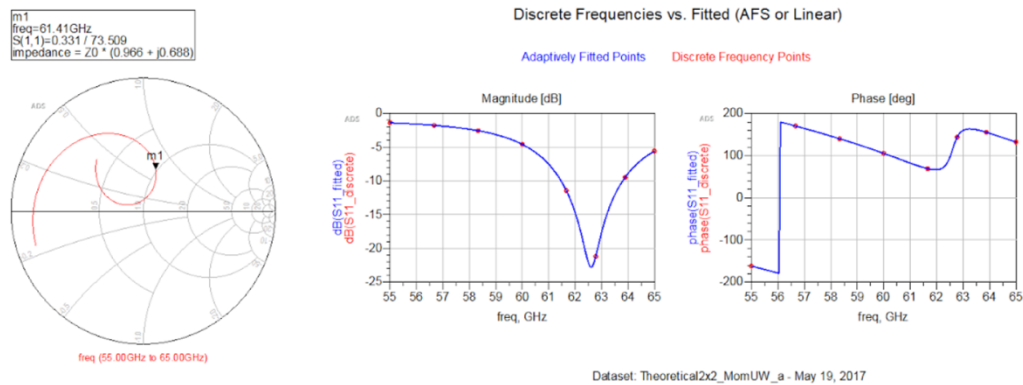
Figure 3.18: Designed 2x1 Patch in ADS Results

The results are shown in figure 3.18. The patch resonates slightly higher than 61 GHz with an S11 of -23.2 dB. This is similar to the results of the surveyed 2x1 patch antenna in the previous section, which resonated at 62 GHz with an S11 of -21.5 dB. The simulated input impedance is 59.3 Ω but for ease of theoretical calculation in the array value of 50 Ω is used to quickly build the feed for the 2x2 patch array.

The 50 Ω input for the 2x1 patch array is fed by a quarter wave transmission line that is intended to terminate at 100 Ω ("a" in figure 3.19). With 2 of these 2x1 arrays together, this junction should be a 50 Ω input impedance which can then be fed by a 50 Ω quarter wave transmission line ("b" in figure 3.19).
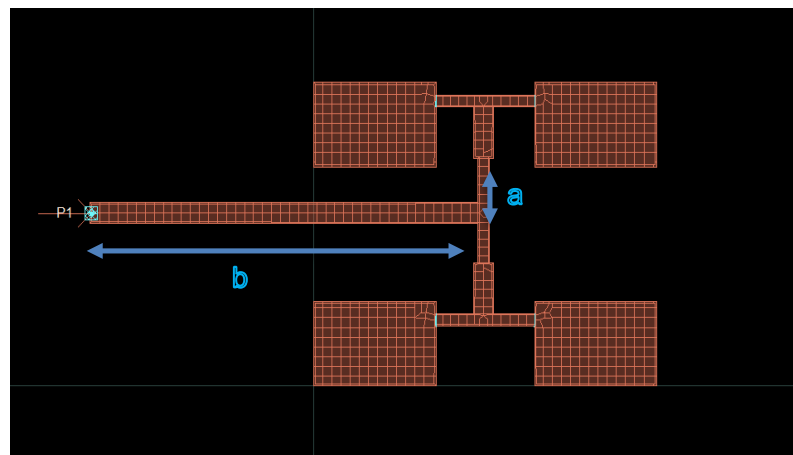
Figure 3.19: Designed 2x2 in ADS
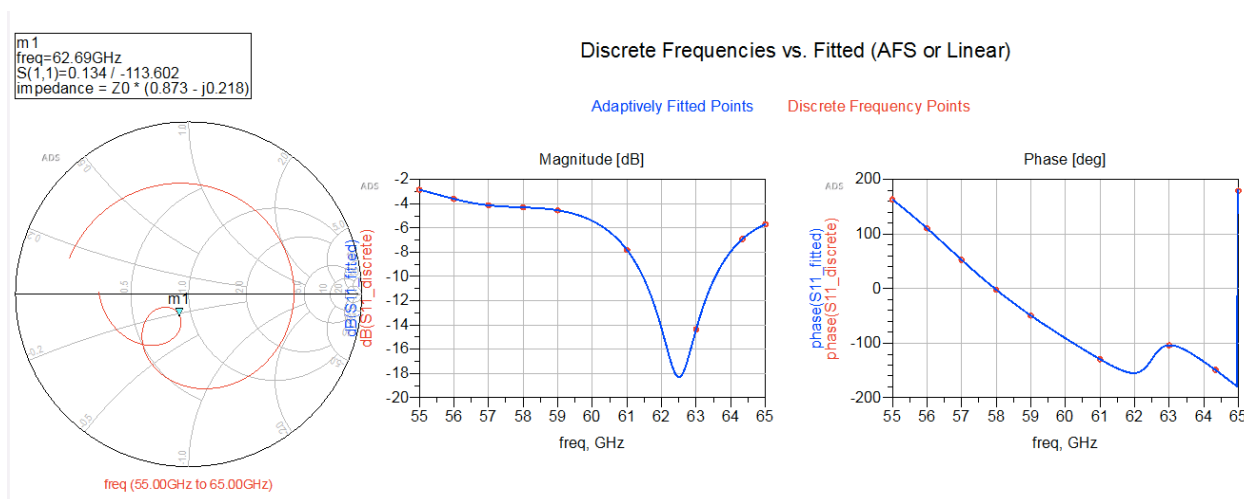
Figure 3.20: Designed 2x2 in ADS Results

Transmission line "a", which has an input impedance of 50 Ω and a load impedance of 100 Ω, has a characteristic impedance of 70.7 Ω which means the dimension of the transmission line is 0.213 mm x 0.931 mm. Transmission line "b" is a straight 50 Ω feed that connects to the 50 Ω input port. The results in figure 3.20 show that the patch array resonates at 62.5 GHz with an S11 of -18.2 dB. The results of the Surveyed patch array and the designed patch array are shown below in table 3.2.

	Surveyed 2x2 Antenna	**Designed 2x2**
Resonant Frequency	61.6 GHz	62.5 GHz
S11	-30 dB	-18.2 dB
Gain	12.8 dB	12.4 dB
Directivity	14.1 dB	13.9 dB
Efficiency	74.1%	71.2%

Table 3.2: Surveyed 2x2 vs Designed 2x2 Patch Results

From looking at these results it can be seen that although we have close results, with slightly higher resonant frequencies and comparable gain, directivity and efficiency values, this indicates that the 2x2 patch array of reference [8] has been optimized more than our simulated model. The S11 in [8] is much better than the simulated model here while efficiency, gain and directivity are just slightly higher. Therefore the layout parameter of the surveyed model from [8] are chosen as the foundation for further investigation on how cavity backing affects the return loss resonant frequency and radiation pattern.

3.3 Cavity Backed Design and Simulation

The design for the cavity backing follows the procedure report in [11] along with our own fullwave optimized simulations. As discussed in section 2.3, there are a number of different methods for creating cavity backing for an antenna. The least complex involves creating a solid metal casing around the patch to reduce power leakage and increase gain, directivity and bandwidth. This section will go through the single, 2x1 and a 2x2 cavity backed patch antenna designs and simulation.

3.3.1 Cavity Backed Single Patch

As explained in Section 2.3, the optimized ratio for the cavity backing is to have the fencing area 1.8 times further than the dimension of the antenna. With a single patch antenna having the dimensions of 2.3 mm x 1.5 mm, the cavity starts at the dimensions of 4.14 mm x 2.7 mm. The design and results can be seen in figure 3.21 and figure 3.22.
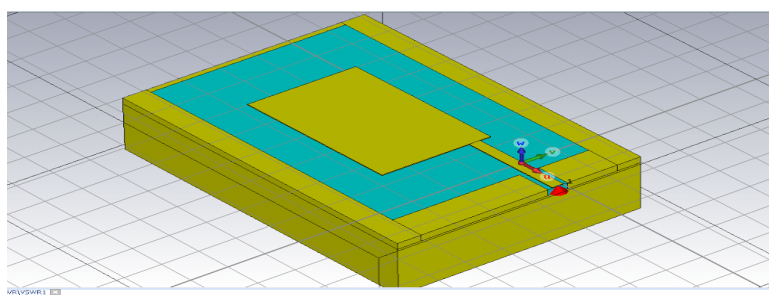
Figure 3.21: Single Cavity Backed Patch
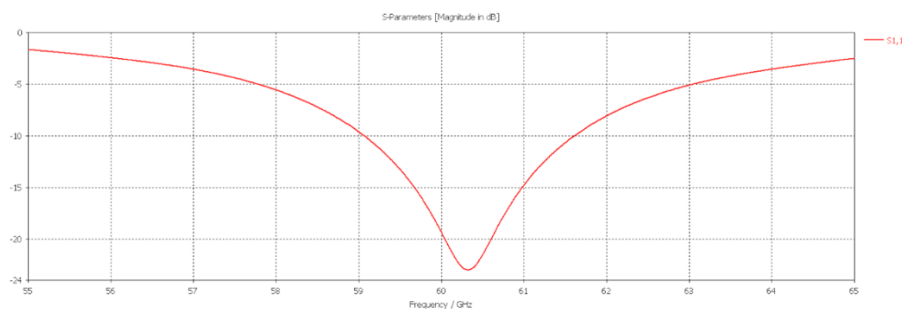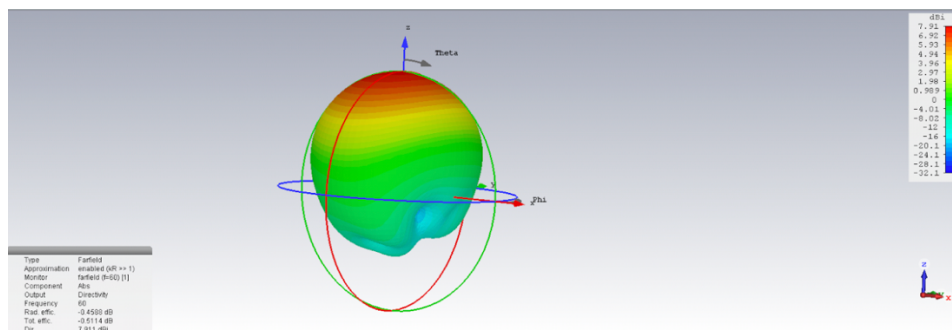
Figure 3.22: Cavity Backed Single Patch Results

The resonant frequency is at 60.3 GHz with an S11 value of -23.3 dB. This is a slightly higher resonant frequency than the single patch without the cavity and a slightly better S11 match. The gain and directivity have also increased from 7.15 dB and 7.6 dBi to 7.45 dB and 7.91 dBi respectively. The 10 dB bandwidth decreased from 3.3 GHz to 2.7 GHz but the all other aspects seem to have been improved. These comparisons can be seen in table 3.3 below.

	Single Patch	Cavity Backed Single Patch
Resonant Frequency	59.8 GHz	60.3 GHz
S11	-18.2 dB	-23.3 dB
Gain	7.15 dB	7.45 dB
Directivity	7.6 dBi	7.91 dBi
Efficiency	88.8%	88.9%
10 dB bandwidth	3.3 GHz	2.7 GHz

Table 3.3: Single Patch vs. Cavity Backed Patch Antenna

3.3.2 Cavity Backed Patch Array

Utilizing the same method, a cavity backing is created for the 2x2 patch array. Each section of the array is fenced with a distance of 1.8 times the length of the section with the larger of the sections taking precedence when the cavity surroundings overlap. The design and results can be seen in figure 3.23 and figure 3.24.
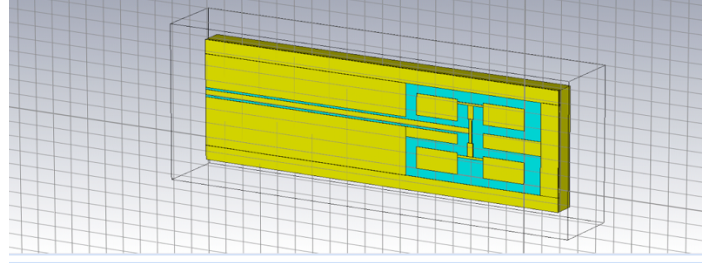
Figure 3.23: 2x2 Cavity Backed Patch
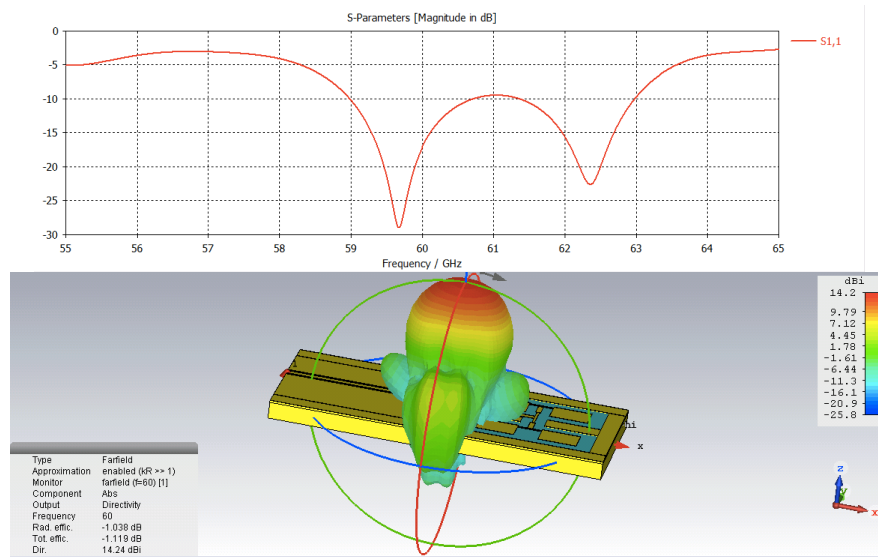
Figure 3.24: 2x2 Cavity Backed Patch Results

The results show that there seems to be two major points of resonance, one at 59.7 GHz and one at 62.3 GHz. The 10 dB bandwidth spans between 59 GHz and 63 GHz which is about .3 GHz more than the non-cavity backed array. The return loss is -28.2 dB and the efficiency is 87.2%, both of which are improvements on the normal patch array. Again the gain and directivity are also both improved, with 12.9 dB and 14.1 dBi respectively. These results are shown in table 3.4 and it seems that the full metal cavity backing again provides improvements in many patch antenna array characteristics.

	2x2 Array	Cavity Backed 2x2 Array
Resonant Frequency	61.5 GHz	59.7 GHz
S11	-26.9 dB	-28.2 dB
Gain	12.6 dB	12.9 dB
Directivity	13.9 dBi	14.2 dBi
Efficiency	79.5%	87.2%
10 dB bandwidth	3.7 GHz	4 GHz

Table 3.3: 2x2 Array vs. 2x2 Cavity Backed Array

3.4 Conclusion

After deconstructing and analyzing the surveyed 2x2 patch antenna along with a designed model, we can see how the different array patterns compare and how optimization can affect the various antenna characteristics. The 2x2 patch array had a much better S11 value, and increased the gain and directivity by around 5 dB compared to the single patch. The S11 bandwidth also increased slightly. The surveyed analysis also performed more desirably than the designed model, most likely due to the optimization of the design. The solid cavity backing also increase antenna gain, directivity and S11 matching while also improving efficiency and S11 bandwidth in the 2x2 case, displaying the possible benefits of utilizing a cavity backing. The cavity has been shown to have major impacts on the return loss vs. frequency spectrum and radiation pattern, implying that different cavity designs could have significant effects on the antenna's operational characteristics. The cavity design used thus far is also an ideal cavity for containing the radiation losses, however it is not necessarily practical for many applications.

Chapter 4 Antenna Design at 60 GHz On R04350

Due to design constraints and for future integration of the array with a phase shifting platform, a second substrate material Roger's 04350 was considered to evaluate the design of patch antennas discussed in previous sections. The R04350 dielectric has a height of .508mm, a dielectric constant of 3.66 and a loss tangent of .0037. This new material has a greater dielectric constant than the Duroid 5880 (3.66 to 2.2), a greater loss tangent (.0037 to .0009) and has a greater height (.508mm to .127mm). Using a new substrate requires a redesign of the layout of the antenna and feed network, but also provides further validation of the various designs methodologies and results reported in Chapter 3. This chapter follows the design and simulation process for creating a microstrip fed 2x2 patch array with cavity backing similar to what was presented in Chapter 3.

4.1 Single Patch Antenna Design and Simulation

Before jumping into the 2x2 array design, a basic patch antenna is designed and analyzed. Utilizing the theoretical formula discussed in Chapter 2 the dimensions of the patch antenna are calculated to be 1.64 mm x 1.02 mm for this new substrate which is a 191% increase in surface area compared to the design reported in section 3.1.2. The design and simulation of this patch in ADS is shown in figures 4.1 and 4.2.
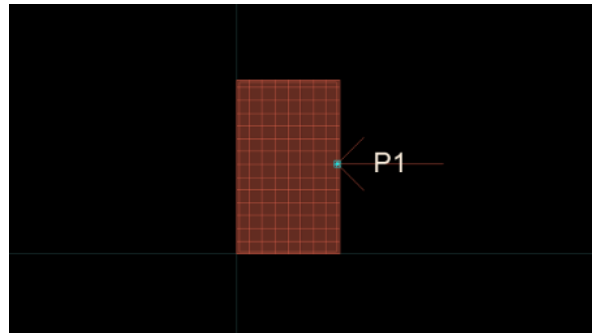
Figure 4.1: Single Patch ADS Rogers
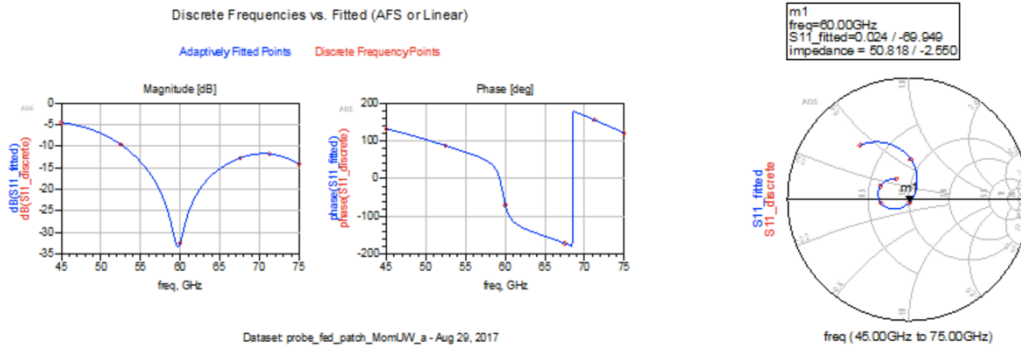
Figure 4.2: Single Patch ADS Rogers

The simulation results show that the patch resonates right at 60 GHz with a return loss of -33.4 dB. According to the theoretical calculations the input impedance should be 209.7 Ω but the simulation results show that the impedance at this point is 51.6 Ω , matching really well with the 50 Ω feeding cable. This inconsistency is investigated further in the next chapter, but for now the result is accepted and the design process is continued.

4.2 Patch Array Design and Simulation

After designing the single patch at 60 GHz the array is built out with quarter wave transmission lines to eventually match the 50 Ω input at P1 shown in figure 4.3. The theoretical input impedance for the patch antenna is 195 Ω . So from the patch, there is a transmission line with a characteristic impedance of 139.678 Ω and a quarter wave of width .086 mm ("a" in figure 4.3), creating a load impedance of 100 Ω . Since there are two transmission lines meeting at this junction, the total impedance at this point is 50 Ω . From here a quarter wave transmission line with a characteristic impedance of 98.742 Ω is utilized to create another 195 Ω load impedance ("b" in figure 4.3). Another 139.678 Ω quarter wave transmission line is used to create a load impedance of 100 Ω , and a total junction impedance of 50 Ω ("c" in figure 4.3). A 50 Ω impedance quarter wave transmission line would be ideal to insert here, which would create a 50 Ω input to match the 50 Ω port input, but the width of this transmission line would be too large and overlap with the patches. This requires another set of transmission lines to clear the patches. A 98.742 impedance quarter wave transmission line ("d" in figure 4.3) connected to a 139.678 Ω transmission line ("e" in figure 4.3) creates a 100 Ω input. From here a quarter wave transmission line with a characteristic impedance of 70.7 Ω is used to create a 50 Ω input to match with the port ("f" in figure 4.3).
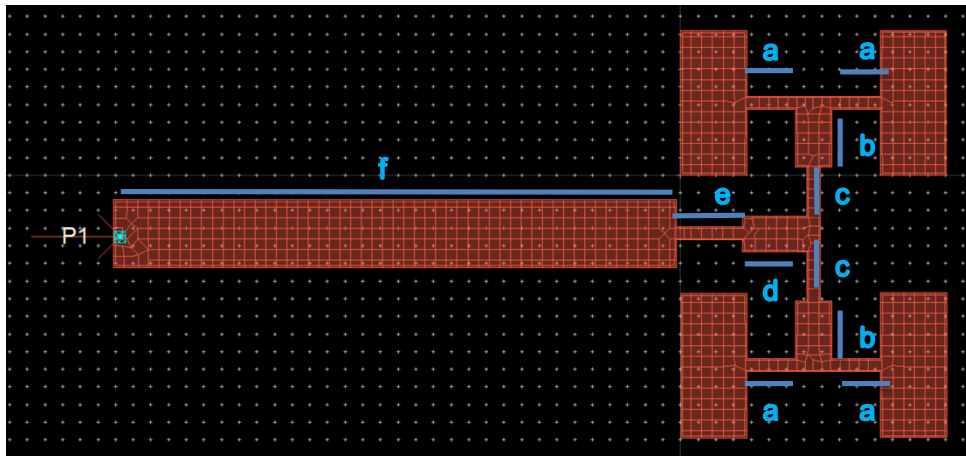
Figure 4.3: 2x2 Patch Array in ADS on R04350

The patch size has been optimized through a parametric sweep to get the ideal resonant frequency. These results are shown in figure 4.4 below.
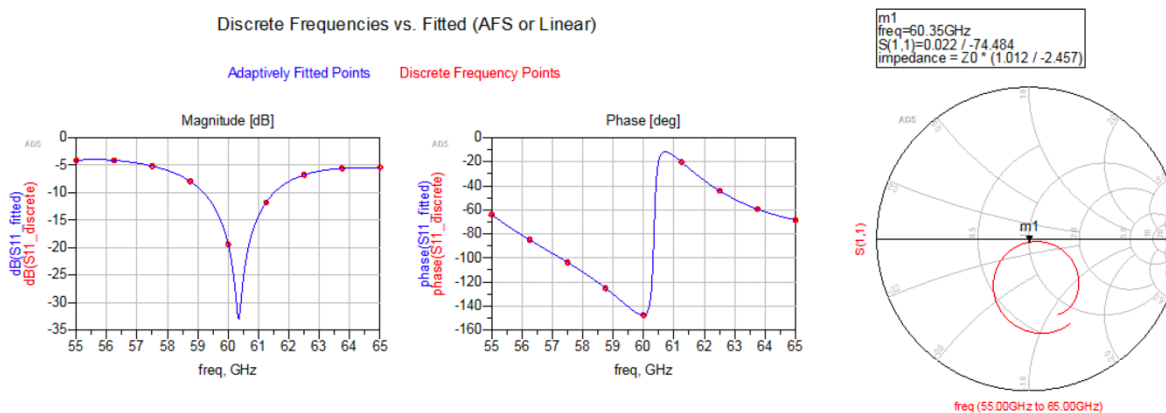
Figure 4.4: 2x2 Patch Array in ADS on R04350 Results

The patch resonates at 60.5 GHz with a return loss of -32.3 dB. At 60 GHz the return loss is -19.3 which is still reasonable and the impedance is 50.6 Ω which is a very good match with the 50 Ω port impedance. A probe fed antenna is designed in Chapter 5 which eliminates the need for the extraneous feeds that could radiate and deteriorate radiation pattern.

4.3 Cavity Backed Design and Simulation

To create the cavity backing the same techniques used in section 3.3 and described in section 2.3 are used here. Figure 4.5 and figure 4.6 show the design and results from CST simulations. Via fence walls are placed around the antennas and feed line as can be seen in the top view shown in figure 4.5. Instead of a completely solid cavity backing, a thin fencing has been used to create the cavity. This is a more realistic and feasible design than a solid case around the entire antenna. This emulates an idealized version of a via fencing.
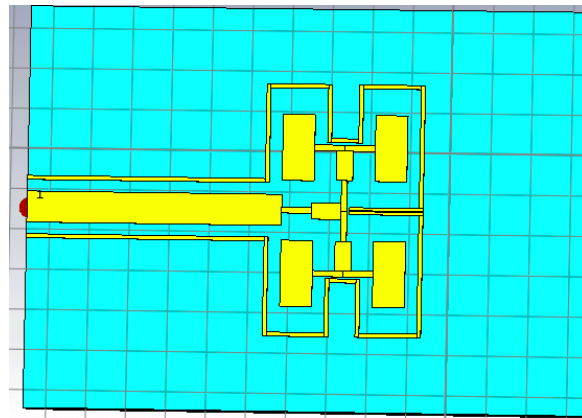
Figure 4.5: 2x2 Array in CST on R04350
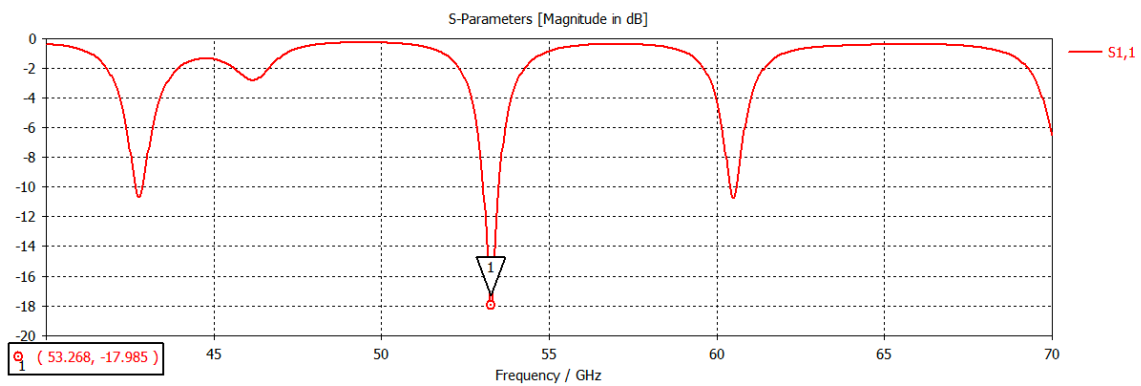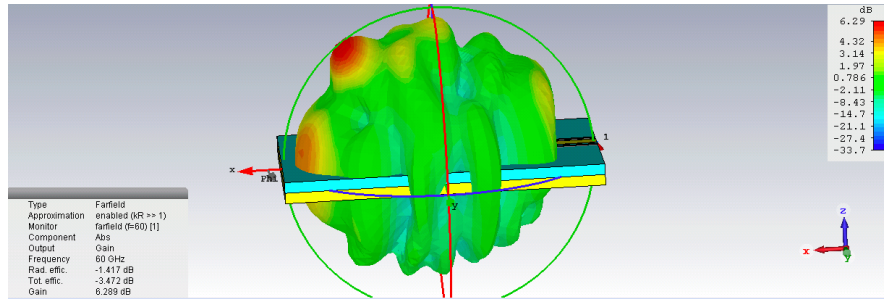
Figure 4.6: 2x2 Array in CST on R04350 Results

Adding the via cavity around the antenna array and feed resulted in the resonance frequency of 53.268 GHz and return loss from of -17.985 dB. The gain and directivity are 6.289 dB and 7.7 dBi, respectively, and the front to back lobe ratio of 7.7 dB is achieved. The radiation pattern shows a beam angle that is not in broadside direction, this is an artifact of radiation of large feed network and radiation of microstrip lines. For this reason elimination of the microstrip and use of probe feeding technique is undertaken in the next chapter.

As a final discussion the Table 4.1 compares the radiation parameters for the 2X2 antenna arrays studied in Section 3.3 and Section 4.3 which indicate a superior design for the antenna array from Section 3.3.

	Cavity Backed 2x2 Array from Section 3.3	Cavity Backed 2x2 Array from Section 4.3
Resonance Frequency	59.7 GHz	53.27 GHz
S11	-28.2 dB	-17.98 dB
Gain	12.9 dB	6.29 dB
Directivity	14.2 dBi	7.7 dBi
Efficiency	87.2%	67.1%
Front to Back Lobe Ratio	18.8 dB	7.7 dB

Table 4.1: 2x2 Array vs Cavity Backed Array on R04350

4.4 Conclusion

Utilizing the new R04350 substrate, an optimize a 2x2 patch array antenna in ADS was achieved. The transmission line fed antenna resonated at 60.5 GHz with a return loss of 32.3 dB. Running the same design in CST even with cavity backing showed a drop in resonance frequency for a few GHz, and decreased the return loss to 18.0 dB. The bulky feed network resulted in deteriorating the pattern so in the next section a probe fed patch array is designed to get around these issues.

Chapter 5 Probe-fed Antenna Design At 60 GHz On R04350

The CST simulations in the previous chapter resulted in less than ideal antenna operations. The transmission line feeds created unwanted losses and the dimensions of the array made it difficult to create an optimized design. To get around this, a probe fed patch antenna is investigated in this chapter. The probe will eliminate the need to use excessive transmission lines to feed the patch antennas. This design iteration is implemented using R04350 dielectric and starting from a single patch design and analysis and extended to a 2X2 patch array design and analysis.

5.1 Single Patch Antenna Design and Simulation

Designing a probe-fed single patch antenna involves first creating an optimized patch antenna layout at 60 GHz then finding the location on patch where the impedance is equal to 50 Ω so that it can be used as the feed point. In Section 4.1 a single patch antenna has already been constructed on the R04350 material so the next step is to use the known equations along with parametric sweeps to find the ideal location for the feed to be inserted. The formula and technique discussed in Section 2.2.2 indicate that the pin should be located at 1/3 of the L length of the patch antenna. We saw some interesting results in section 5.1 where the input impedance of the patch seemed to match to 51.6 Ω at the center edge of the patch. The pin input can also be used to model a probe feed in ADS and the design and results are shown in figure 5.1. It can be seen that the patch resonates well at 60 GHz with -33.6 dB return loss and an impedance of 50.82 Ω .
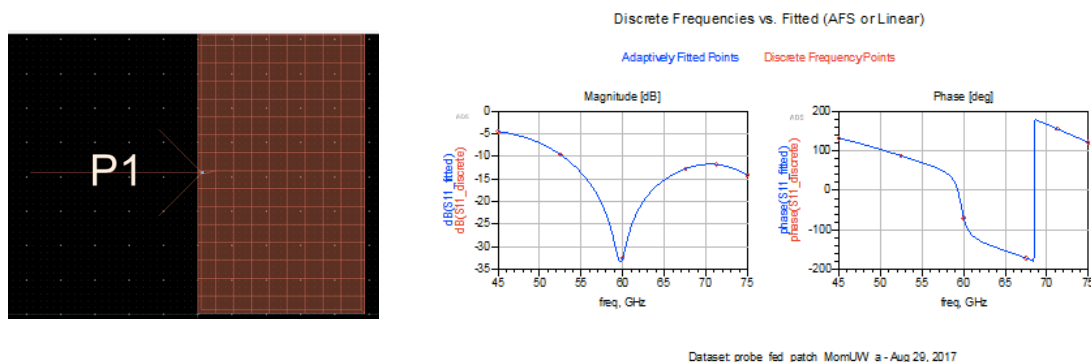
Figure 5.1: Probe-fed Single Patch in ADS

Theoretically this impedance should have been closer to 209.7 Ω . Therefore, a thorough parametric sweep is done to see if these results hold up in CST. To create the probe in CST a cylindrical conductor is burrowed through the dielectric and fed by a waveguide port. There is a

circular separation from the ground plane (a.k.a. ground clearance) to allow current to flow to the antenna. This design in shown in figure 5.2 below.
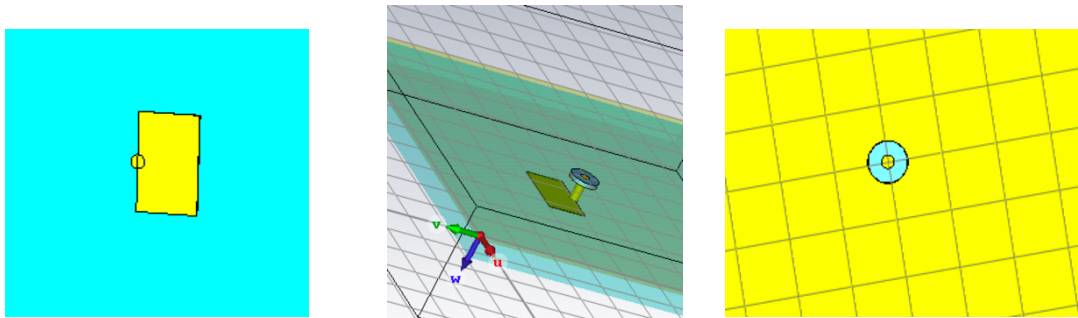
Figure 5.2: Probe-fed Design

A parametric sweep is utilized to determine the optimal dimensions of the patch antenna. The length of the patch is varied from 0.8 mm to 1.1 mm with 15 samples, the location of the probe input is varied from 0 to 0.4 mm with 6 samples and the width is varied from 0.79 to 0.83 mm. This parametric study is meant to give a thorough analysis of the possible design dimensions. The results of this parametric sweep are shown in figure 5.3 below.
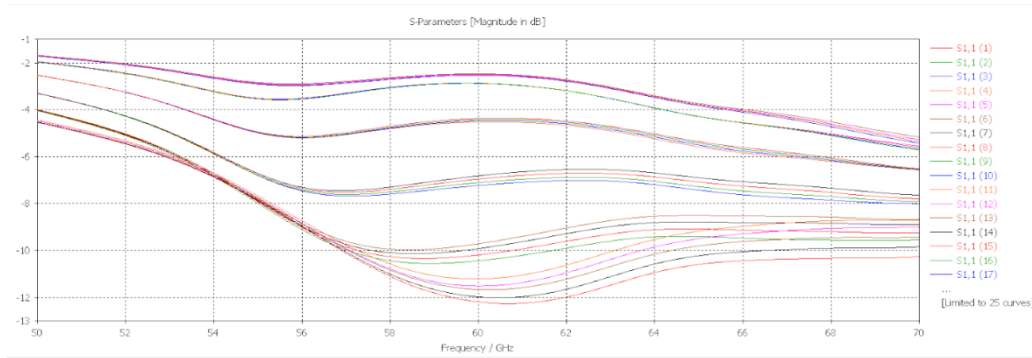
Figure 5.3: Single Patch Probe-fed Parametric Sweep

There is a pretty clear correlation between probe location and impedance matching as 6 distinct groupings can be seen despite the variations in length and width. The probe location closest to the edge, at 0 mm, matches the best while the probe location at 0.4 mm has the worst match. This is a very interesting outcome as it confirms ADS simulation but goes against the closed-form formulas for finding the appropriate feed location to match to a 50 Ω input.

After confirming the location of the input probe, further parametric sweeps are done to narrow down the ideal dimensions for the length and width of the patch. After many simulations to pin point the patch to operate at 60 GHz the dimensions of W = 0.82 mm and L = 1.033 mm gives the best results, shown in figure 5.4 The patch resonates at 60.2 GHz with a return loss of -35.9

dB and a gain of 6.11 dB and a half-power beam width (HPBW) of 71.2 deg. The S11 BW is 15.1 GHz and the front to back lobe ratio (FTBLR) is 10.8 dB.
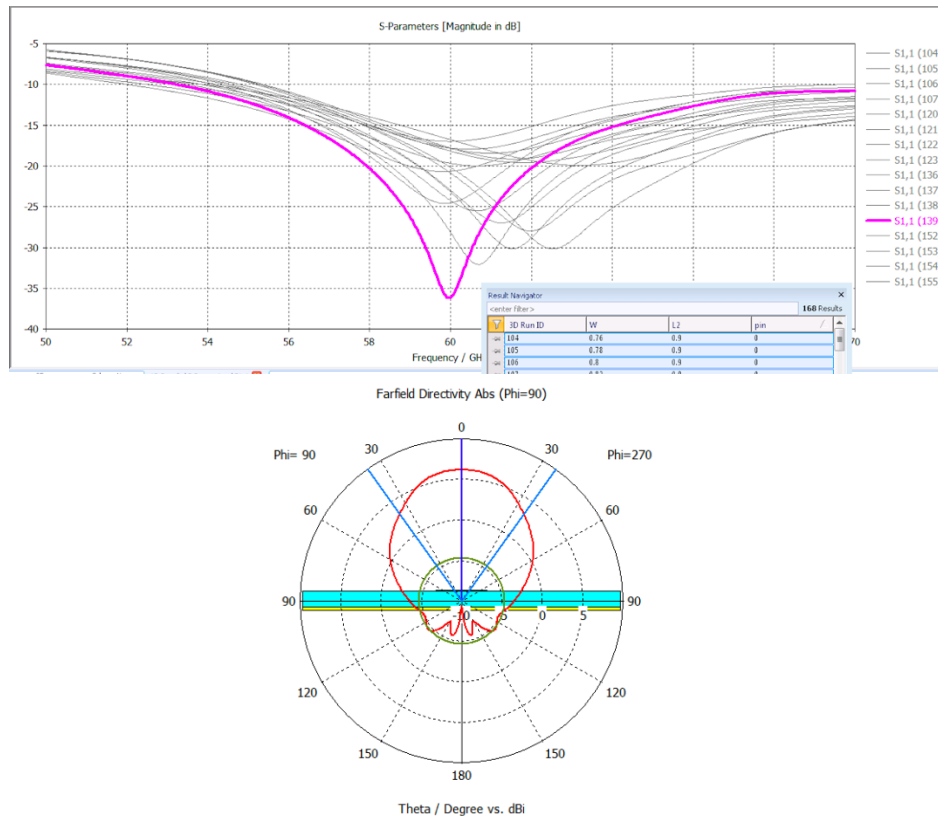
Figure 5.4: Single Patch Probe-fed Results

These results are pretty good for a single patch antenna and closely match the ADS results. Now that the single patch antenna is optimized, a patch array can be constructed.

5.2 Patch Array Design and Simulation

To create the first iteration of the 2x2 probe-fed patch antenna the patch array design from section 5.2 is utilized. The P1 input junction has a theoretical impedance of 50 Ω and can be used as the input point for our probe feed. The ADS design and its simulation results can be seen in figure 5.5.
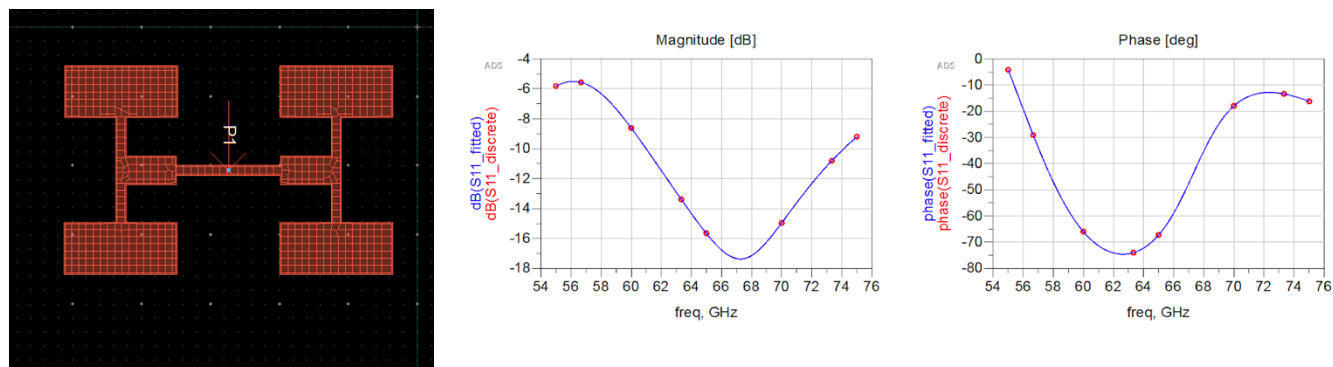
Figure 5.5: Probe-fed Patch Array #1

This design still has high variations in impedances, transitioning from a 139.68 Ω , to a 98.79 Ω then back to a 139.68 Ω impedance transmission line from patch to feed. These fluctuations in impedances cause more losses and excite surface waves which decrease the efficiency of the patch. After multiple iterations and simulations, a more effective design is created in CST. This design is intended to create a better transition between transmission line impedances from patch to feed. Since we are using a probe-fed technique, we have more room to work with and more options for creating a feed system that flows from low to high impedance, instead of high, low then high like the previous design.

The design for the optimized 2x2 patch antenna went through multiple iterations and required some parametric sweeps to get the ideal dimensions, but the finalized design is shown in figure 5.6 below and the results are shown in figure 5.7. The input of each patch has an impedance of 50 Ω , as seen from previous sections, and the desired load impedance for section "a" is 250 Ω . This leads to section "a" having the dimensions of 0.297 x 0.739 mm and a characteristic impedance of 111.924 Ω . This leads to the junction with section "b" having an impedance of 125 Ω . The desired impedance leading into section "c" is 75 Ω so section "b" has the dimensions 0.427 x 0.728 Ω and a characteristic impedance of 96.842 Ω . To create the last section, connecting to a 50 Ω feed, the desired impedance from each transmission line should be 100 Ω . This leads to the dimensions of 0.297 x 0.739 mm for section "c" and a characteristic impedance of 86.618 Ω.

$$a = 0.297 \times .739$$
$$c = 0.427 \times 0.728$$
$$b = 0.539 \times 0.72$$
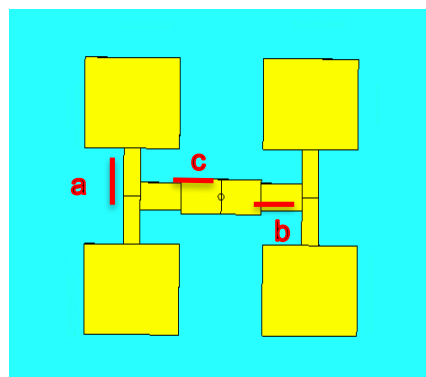
Figure 5.6: Probe-fed 2x2 Patch Array #2
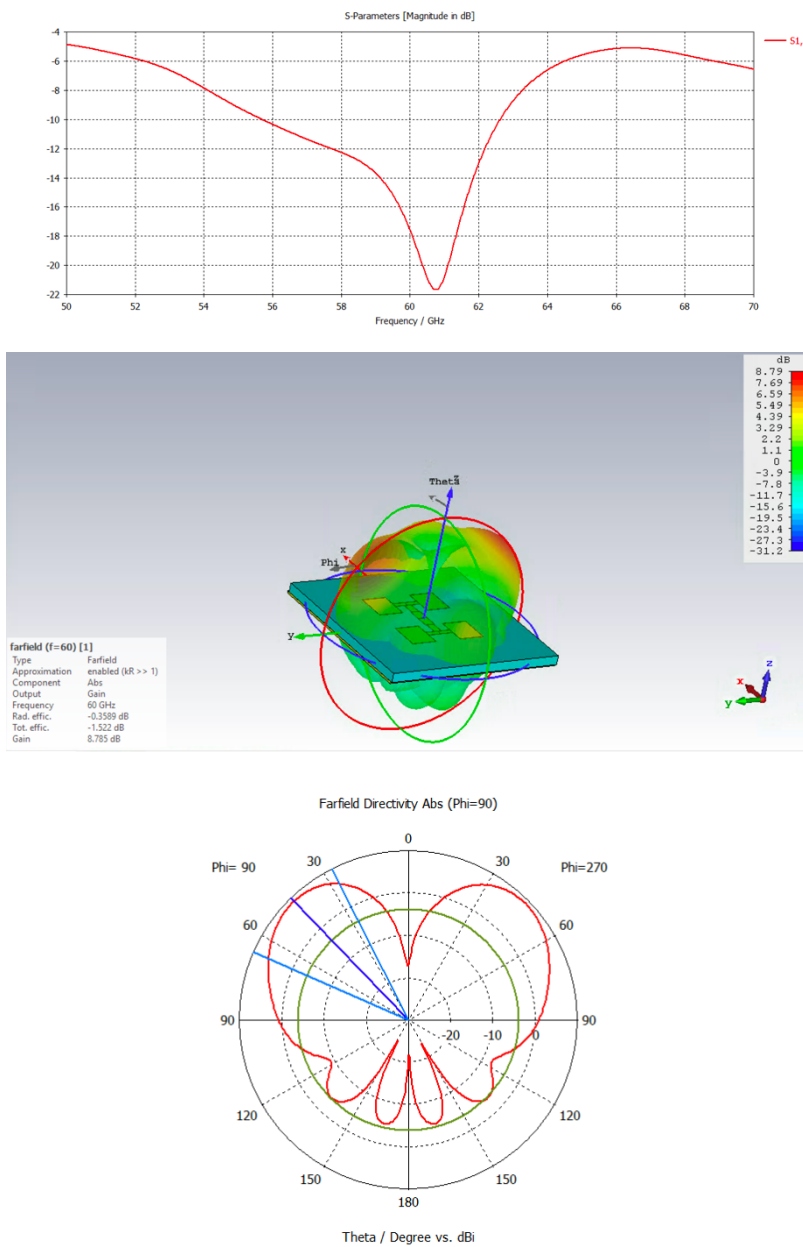
Figure 5.7: Probe-fed 2x2 Patch Array Results

The simulation results depicted in figure 5.7 show that the patch resonates slightly high, at 60.7 GHz, with a return loss of -21.9 dB. At 60 GHz the return loss is -18 dB and a gain of 8.6 dB. The HPBW is 39.5 degrees and the FTB lobe ratio is 12.82 dB. These results show that the 2x2 patch array has a 2.5 dB increase in gain but the results state that the HPBW has decreased by 31.7 degrees. When looking at the actual farfield radiation pattern, however, this HPBW value is a bit skewed. There are actually 2 main lobes for the 2x2 patch array, both of which have a HPBW of 39.5 degrees, creating a much wider range than the single patch antenna. There is also a notable null directly above the patch which we would not typically expect for a 2x2 patch array.

This null is most likely due to the feed design, as the distance between patches are not a factor considering they are less than a single free space wavelength apart. Despite the dual lobe effect, these results are much better than the transmission line fed 2x2 patch array antenna of section 4.2. This probe fed 2x2 patch array has a better return loss (-17.475 dB improvement) and resonates much closer to the desired 60 GHz. The next step is to create a cavity backing to optimize the patch antenna performance.

5.3 Cavity Backed Design and Simulation

The cavity backing for the final model is implemented with copper plated via hole fences. These via walls are the most viable and realistic way of creating shielding walls in PCB technology and even in wearable devices which often require flexible or textile substrates. In addition, via fencing has a small footprint, and can be integrated into circuitry more efficiently than solid copper fencing. The process for designing a via fence involves first determining the ideal hole diameter and spacing between holes. Next, as before the spacing between via fence walls around a single patch should be determined the save way cavity backing was designed in previous chapters. Initial designs are done in ADS as the process of creating and editing multiple via's is much simpler in ADS. The designs are then exported to CST and adapted to the 3-D model and further simulations are conducted. After creating a finalized design for a single patch the process is repeated for a 2x2 path array.

5.3.1 Single Patch Via Fence Cavity

In order to determine the diameter of the via (D) and the spacing between them (S) the technique discussed in Section 2.3 is utilized. According to the optimized ratio for a similar dielectric material which is D = 0.059 λ and S = 0.14 λ, from reference [11] D = 0.2 mm and S = 0.472 mm for R04350 is found for our design. Figure 5.8 show the created cavity backed single patch antenna layout in ADS.
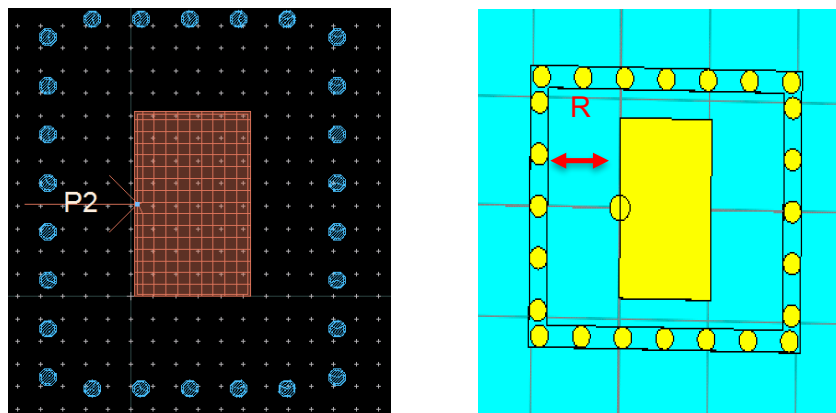
Figure 5.8: Single Patch Via Fence In ADS and CST

This model is then exported to CST for parametric sweep simulations. From Section 3.3 the optimized dimension for the cavity width (R) is 1.8 times the length (L) of the patch antenna. Initial fullwave simulations did not support this point. Multiple parametric sweeps of the cavity length and width as well as the patch length and width is needed to narrow down the variables to create a patch that resonates well at 60 GHz. Similar to previous simulations, the cavity has major effects on the radiation pattern and antenna characteristics but the pattern seems to hold true to a degree. From these simulations it seems that the width of the cavity has more of an influence on the general shape of the return loss, including resonance frequency, while the length of the cavity has more of an influence on the magnitude of the return loss, bringing S11 up or down or sharpening certain resonance points. Figure 5.9 demonstrates this phenomenon.
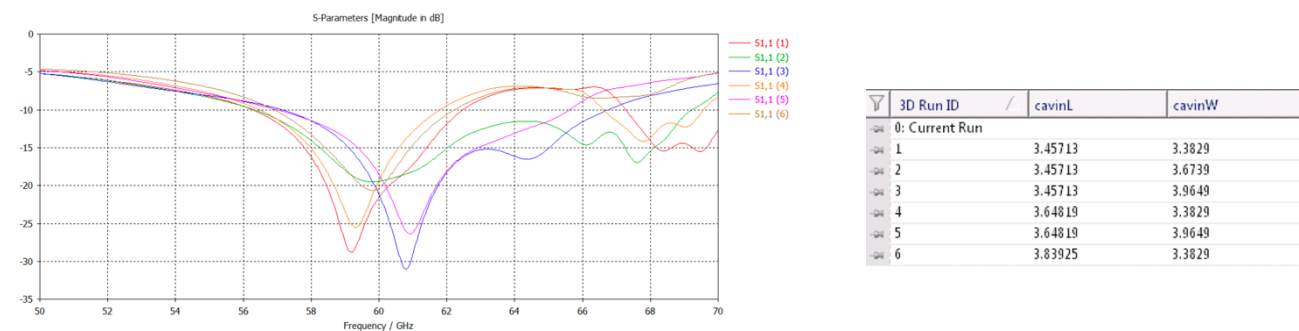
Figure 5.9: Effect of Cavity Length vs. Width

There are 3 distinctly different S11 curve signatures in this figure corresponding to the 3 different cavity width values. There are also distinctly different resonance frequencies for these curves and the cavity length tinkers with the S11 magnitude at the different resonance points. Looking at curves 2 and 3, the cavity length is identical at 3.46 mm but the curves do not resemble each other at all. This is because the cavity width varies from 3.67 mm to 3.96 mm. Curves 3 and 5, however, look very similar except for the S11 values associated with them. These curves both have a cavity width of 3.96 mm but have varying cavity lengths from 3.46 mm to 3.65 mm.

Eventually an optimized design is found for the single patch antenna. The cavity dimensions are 2.16 x 2.67 mm which means the spacing between patch edge and cavity is CW=0.26 mm and CL=0.82 mm. This is shown in figure 5.10 below with the results in figure 5.11.

Patch: 1.64 x 1.03 mm
Cavity: 2.16 x 2.67 mm
CWxCL: 0.26 x 0.82 mm
Via Diameter: 0.2 mm
Via Spacing: 0.47 mm
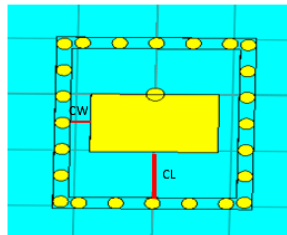
Figure 5.10: Single Patch Via Fence Dimensions
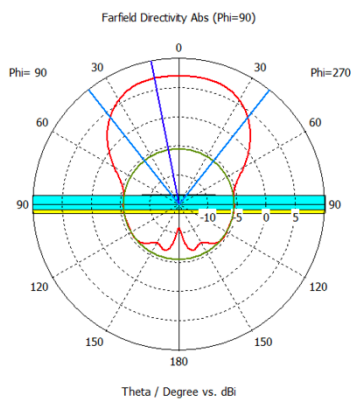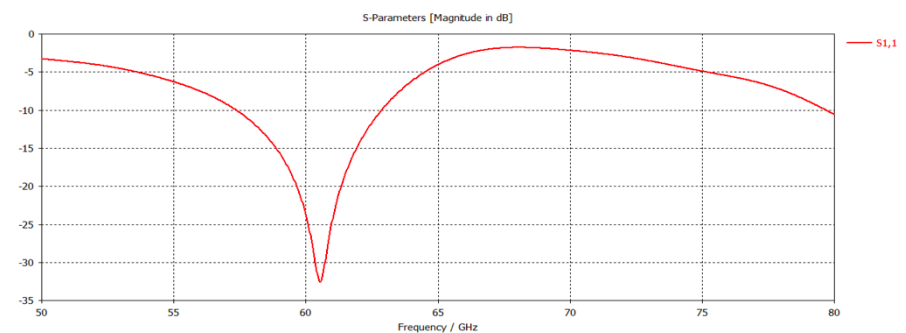
Figure 5.11: Single Patch Via Fence Results

The antenna resonates slightly higher, at 60.8 GHz, with a return loss of -33.4 dB. At 60 GHz the return loss is -24.4 dB and the gain is 6.11 dB which are excellent results for a mm-wave design. The HPBW is 76.5 degrees and the FTBLR is 12.55 dB. This represents a 0.83 dB increase in gain and a 5.3 degree increase in HPBW from the single patch without the cavity. The S11 -10

dB bandwidth is 5.5 GHz which is 9.6 GHz narrower compared to the patch without the cavity in section 5.1. The FTB ratio is also improved by 1.75 dB. The via fencing has successfully improved many characteristics of the patch antenna and has created a narrower bandwidth at 60 GHz. The next step is to create a cavity backing by using via fences for the 2x2 patch antenna.

5.3.2 Patch Array Via Fence Cavity

Similar to the single patch via fence, the patch array via fencing does not conform to the surveyed ratio. As such, a litany of simulations is required to find the optimal design. The design of the patch array also results in a full rectangular via fence cavity as opposed to the component outlining implemented with via fences implemented in the microstrip fed array cavities discussed in Chapter 4. The final cavity has 6.76 x 6.91 mm cross section area which results in the spacing between patch edge and cavity being CW = 0.93mm and CL = 1.21 mm, as shown in figure 5.12. The results are also presented in figure 5.13.

Patch: 1.5 x 1.7 mm
Cavity: 6.76 x 6.91 mm
CWxCL: 0.93 x 1.21 mm
Via Diameter: 0.2 mm
Via Spacing: 0.47 mm
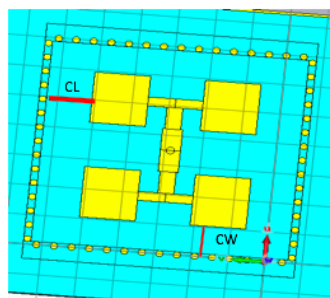
Figure 5.12: Patch Array Via Fence Dimensions
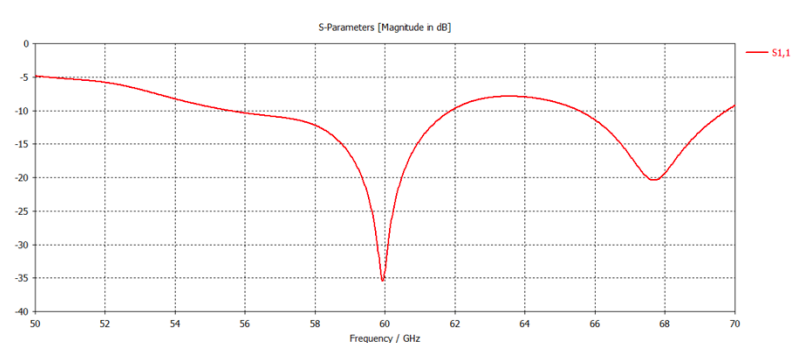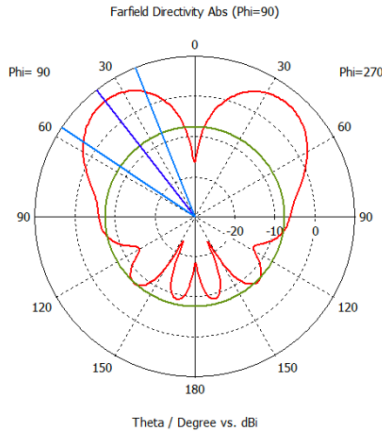
Figure 5.13: Patch Array Via Fence Results

This patch array with via fence walls resonates right at 60 GHz with a return loss of -35.1 dB and a gain of 7.2 dB. The HPBW for each radiating lobe is 34.3 degrees which is 5.2 degrees less than the patch array without the cavity. Like the 2x2 array there are 2 main lobes due to the feed design, so this value is a little skewed. The S11 -10dB BW is 5.8 GHz which is 1.1 GHz narrower than the 2x2 patch of section 5.2 and the FTBLR is 14.06 dB which is a 1.24 dB improvement on the 2x2 patch. The patch array is again successfully improved by the via fence cavity backing.

5.4 Conclusion

In this section a via fence cavity backing was designed and successfully improved the performance of a single patch and a 2x2 patch array. The surveyed via fence spacing ratio of R = 1.8a did not hold for this design and so a multitude of simulations and parameter sweeps were performed to find the best cross sectional area for the cavity. The final design for the single patch had a via cavity with a total width of 2.16 mm which is 1.32 times the patch width and a via cavity with a total length of 2.67 mm which is 2.59 times the patch length. For the 2x2 patch array a rectangular via fence cavity encases the entire array with the cross sectional area of 6.76 x 6.91 mm. The spacing between patch edge to cavity walls ends up being 2.24 times the width of the patch and 2.42 times the length of the patch. The via fence cavity had major effects on the radiation pattern and resonance frequency, It was observed that the width of the cavity had more impact on the general shape of the return loss curve while cavity length altered the S11 depth and matching of the patch. For both single and 2x2 patch cavities the FTB lobe ratio was improved, with varying effects on gain, HPBW and S11 BW. The full results can be seen in Table 5.1.

Antenna	Gain	HPBW	S11 BW	FTB Ratio
Single	6.11 dB	71.2 deg	15.1 GHz	10.8 dB
Single w/ Via	6.93 dB	76.5 deg	5.5 GHz	12.55 dB
2x2	8.6 dB	39.5 deg	6.9 GHz	12.82 dB
2x2 w/ Via	7.2 dB	34.3 deg	5.8 GHz	14.06 dB

Table 5.1: Single and Array Comparison With and Without Via

Chapter 6 Sample Application: Vital Sign Detection

The fundamental theory of Doppler radar remote vital sign detections (VSD) is based on the idea that human breathing and heart beat vibrations will modulate the phase of the backscattered EM waves. These backscattered waves can then be analyzed to extract health information, allowing for non-invasive health monitoring, eliminating the need for physical contact to receive biological data about individuals. One of the first instances of a remote VSD device being utilized dates back to the 1980's when the military developed an X-band microwave life detection system to sense the physiological status of soldiers on the ground in the battlefield [13]. Another system in the 450 – 1150 MHz wave range was utilized to penetrate through earthquake rubble to locate trapped victims during a natural disaster [13]. More recent medical research has been focused around the Ka-Band and further into the 60 GHz range. A few applications for remote VSD are shown in Figure 6.1. This technology has the ability to be integrated into many facets of life, offering convenience, new experiences and lifesaving opportunities.

Figure 6.1: Remote VSD Applications [15]

6.1 Basic Theory

Similar to how the Doppler Effect states that changes in position of the source or observer of sounds waves results in shifts in frequency, periodic movement of the chest cavity results in shifts in phase. Looking at figure 6.2, we can see T(t) is the transmitted signal and R(t) is the received signal, which is a function of T(t) with an added phase shift due to x(t) which represents the sinusoidal motion of the chest cavity. $\varphi(t)$ represents the phase noise generated from the signal source.

$$T(t) = \cos\left[2\pi ft + \varphi(t)\right]$$

$$R(t) \approx \cos\left[2\pi ft - \frac{4\pi d_0}{\lambda} - \frac{4\pi x(t)}{\lambda} + \varphi(t - \frac{2d_0}{c})\right]$$
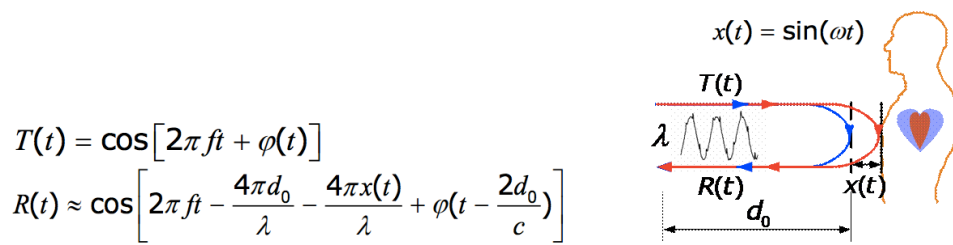
Figure 6.2: Doppler Effect [19]

Knowing the signal generated and the signal received, a directional coupler or mixer can be utilized to generate the f1 + f2 and f1 – f2 signals. This results in the equation:

<div align="right">*Equation 6.1*</div>

$$B(t) \approx \cos\left[\frac{4\pi d_0}{\lambda} + \frac{4\pi x(t)}{\lambda} + \theta_0 + \Delta\phi\right]$$

$\frac{4\pi d_0}{\lambda} =$ Antenna-to-target round-trip delay $\frac{4\pi x(t)}{\lambda} =$ Phase modulation due to chest-wall movement

$\theta_0 =$ Phase delay in receiver circuit $\Delta\phi = \phi(t) - \phi(t - \frac{2d_0}{c})$

Low frequency vitals register between 1-2 Hz so phase noise cancellation is essential in getting accurate data, as small electric phase noise could drastically alter vital signs. According to the range correlation effect, close-in phase noises are correlated and since the same source is utilized for the transmitted signal and the local oscillator signal these factors can essentially be cancelled leaving us with the equation below:

<div align="right">*Equation 6.2*</div>

$$B(t) \approx \cos\left[\frac{4\pi d_0}{\lambda} + \frac{4\pi x(t)}{\lambda} + \theta_0\right]$$

The remaining equation contains a phase component corresponding to the antenna to target delay, a phase component corresponding to phase modulation due to chest movement and phase delay in the receiver circuit. In order to isolate the desired chest movement phase component, a linear approximation is utilized. The small angle approximation states that as an angle approaches zero, $\sin\theta \cong \theta$. If the movement, x(t), of the chest is very small compared to the wavelength of the signal, it is sufficient to use this small angle approximation. The phase delay in the receiver circuit and round-trip delay can be set to 90 degrees to convert the cos function into a sin function and we get:

$$B(t) = \sin\left[\frac{4\pi x(t)}{\lambda}\right] \cong \frac{4\pi x(t)}{\lambda}$$

This formula is now a function of only x(t), the target chest movement. This data can then be further analyzed to get accurate vital sign data. A general setup of this process is depicted in figure 6.3 below.
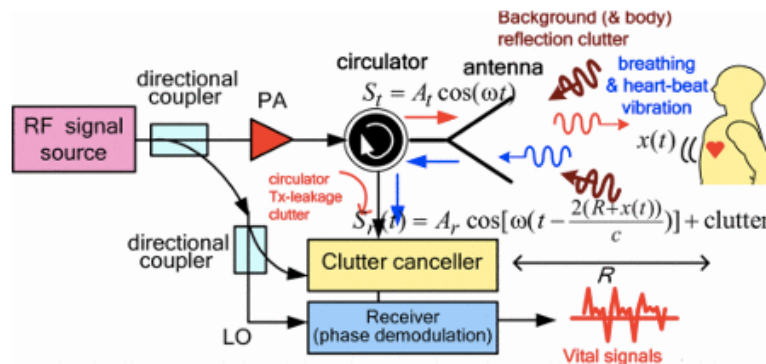
Figure 6.3: Remote Vital Sign Detection Setup [14]

This basic theory sets the foundation for remote VSD but has some limitations. Firstly, this setup does not take into account body movements that may alter the phase modulation of the vital signs. Another drawback of this model is that it requires vital movement to be much less than the signal in order to satisfy the linear approximation. To get better accuracy of data, however, a higher frequency and thus higher ratio of vital sign to signal sign breaks the small angle approximation and different techniques need to be utilized.

6.2 Body Movement Cancellation

To eliminate the effects of body movement, which can cause skewed vital sign data, 2 sensors are utilized: one for the front and one for the back of the patient, as shown in figure 5. Having 2 radars on both sides of the patients means that movements will create opposite effects in each radar. When the 2 signals are combined the body movement will be cancelled out.

Front: $S_f(t) = \exp\left\{ j\left[\dfrac{4\pi x_{h1}(t)}{\lambda} + \dfrac{4\pi x_{r1}(t)}{\lambda} \oplus \dfrac{4\pi y(t)}{\lambda} + \phi_1 \right] \right\}$

Back: $S_b(t) = \exp\left\{ j\left[\dfrac{4\pi x_{h2}(t)}{\lambda} + \dfrac{4\pi x_{r2}(t)}{\lambda} \ominus \dfrac{4\pi y(t)}{\lambda} + \phi_2 \right] \right\}$

x_{h1}, x_{h2}, x_{r1}, x_{r2}: physiological movements

$y(t)$: random body movement
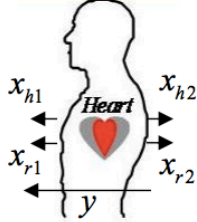
Figure 6.4: Body Movement Cancellation Setup [15]

The front sensor has a positive value associated with the random body movement while the back sensor has a negative value associated with the random body movement. Combining these 2 signals gives us a function that is only dependent on heart rate (h) and respiratory (r) signals.

Equation 6.4

$$S_{fb}(t) = S_f(t) \cdot S_b(t) = \exp\left\{ j\left[\frac{4\pi\left[x_{h1}(t) + x_{h2}(t) \right]}{\lambda} + \frac{4\pi\left[x_{r1}(t) + x_{r2}(t) \right]}{\lambda} + \phi_1 + \phi_2 \right] \right\}$$

Using this two-sensor technique we are effectively able to eliminate body movement variables from vital sign detection and analysis. If the signal to vital sign fits the small angle approximation, then the linear approximation is an accurate depiction of the heart rate and respiratory rate. If the ratio does not fit the approximation, then we must use non-linear techniques to extract the data.

6.3 Non-linear Phase Vital Sign Detection

High frequency VSD provides more accurate data and is much more sensitive to vital sign variations but also requires the use of non-linear techniques as small angle approximations do not hold. Using the Fourier Series we can analyze the signal in frequency domain to determine the heart rate and respiratory rate.

$$x_h(t) = m_h \cdot \sin\omega_h t, \ x_r(t) = m_r \cdot \sin\omega_r t$$

$$B(t) = \cos(\frac{4\pi x_h(t)}{\lambda} + \frac{4\pi x_r(t)}{\lambda} + \phi)$$

$$= \sum_{k=-\infty}^{\infty} \sum_{l=-\infty}^{\infty} J_l(\frac{4\pi m_h}{\lambda}) J_k(\frac{4\pi m_r}{\lambda}) \cos(k\omega_r t + l\omega_h t + \phi)$$
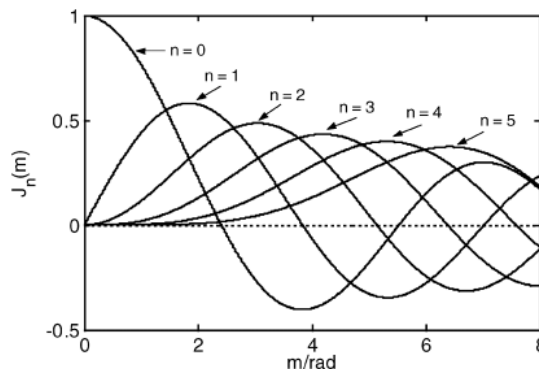
Figure 6.5: Bessel Function [19]

Jn(x) represents the n-th order Bessel function. Bessel's equation can be used to find separable solutions to Laplace or Fourier equations. Using the Bessel harmonics, we can decipher respiratory and heart signals. There can be an issue with Bessel harmonics, however, as some order harmonic of the respiratory signal may overlap with the first harmonic of the heart rate. It often ends up being the case that the 4th harmonic of the respiratory signal is close to the first harmonic of the heart rate and therefore the ratio between the two can determine the impact of the harmonics. A study done in the Ka-band with front and back sensors is shown in figure 6.5.
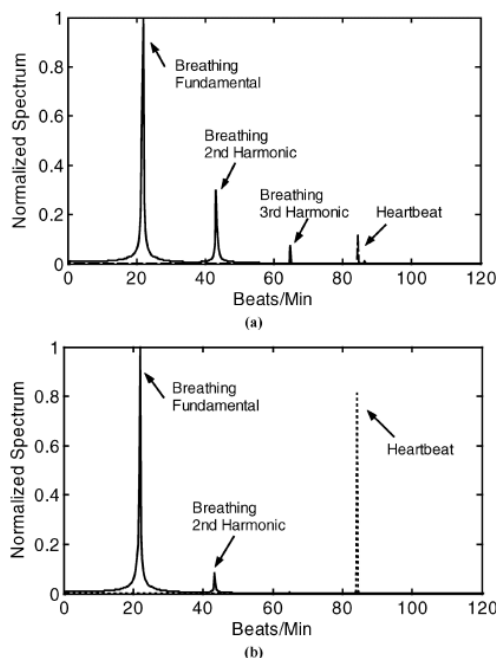
Figure 6.1: Ka-band Study (a = front; b = back) [17]

It can be seen how the first heartbeat harmonic falls very close to the 4th harmonic of the breathing fundamental. It should be noted that the ratio of breathing harmonic to heartbeat harmonic is much more balanced when measuring vital signs from behind the patient. Here, the heartbeat is clearly distinguishable from the harmonics of the breathing fundamental.

6.4 Conclusion

Remote VSD is a technology that has many different applications including security, gaming, health, disaster relief, warfare etc. At low frequencies we can simply utilize a mixer and small angle approximations to abstract phase modulations due to vital signs from backscattered EM waves. In addition, two sensors can be used to cancel out variations due to body movements. At higher frequencies we get much more accurate data due to higher resolution 60 GHz usage would be able to give high precision information and offer science, medicine and other industries a new tool to improve radar, IOT and VSD applications . A patch antenna would be the ideal antenna for VSD applications as it is easily integrated into wearable devices. In addition, using cavity backing technique for patch antennas reduces back radiation and hence user's exposure to electromagnetic waves.

Chapter 7 Investigation for Fabrication

In order to fabricate the antennas a Gerber file with defined design specifications needs to be exported and sent to a fabrication house. Since the final designs are in CST, the 2-D layers need to first be exported into ADS. In ADS the layers and different components are grouped and defined and are then converted to Gerber files. In addition an SMA connector is needed to attach the vector network analyzer (VNA) to the antenna feed. The process and procedure for these tasks are explained in this chapter

7.1 Exporting CST To ADS

The first step in exporting CST designs into ADS involves aligning the axis with the edge of the top plane of the patch. From here select *export → 2D Files → Gerber (Single Layer)* as shown in figure 7.1. The same technique is then applied to the ground plane of the patch antenna to export the design.
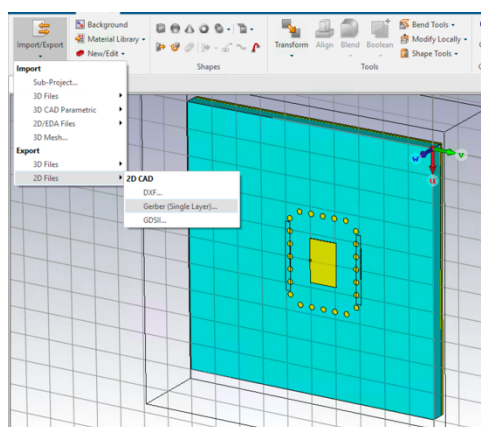
Figure 7.1: Export CST To ADS

In ADS import both layers of Gerber files by selecting *File → Import → Gerber* and selecting the .gbr files, as shown in figure 7.2.
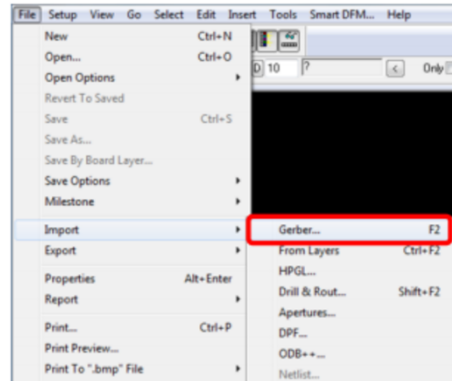
Figure 7.2: Importing To ADS

Then select the various components individually and assign them to their respective layers and give them labels. For example, the patch is on the top layer and the ground is on the bottom layer, both should be copper. The probes are pcvias that connect from top layer to bottom layer and the vias should be a different pcvia that also connects top layer to bottom layer. These pcvias will be copper plated and thus need to be defined as a different set of files.

These steps repeated for all of the designs (single patch, single patch with cavity, 2x2 patch array and 2x2 patch array with cavity). The end design should look like figure 7.3 with all of the associated .gbr files.
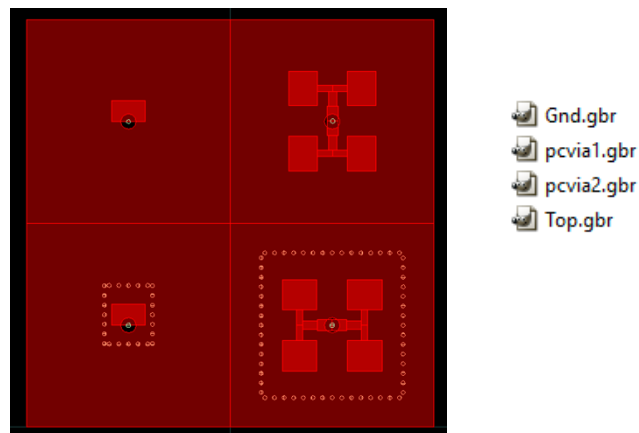
Figure 7.3: ADS Design And Gerber Files

These Gerber files can then be sent to a fabrication house with specifications regarding the different components as well as the dielectric material. The sent design would specify:

- Top and Gnd are copper
- Pcvia1 is just a through hole via
- Pcvia2 are all copper plated via's
- Dielectric = R04350; height = 0.002 inches

A quote for different ordering options is then given to you to choose from when placing the order. In addition to this an SMA connector is also needed.

7.2 SMA Connector

For a 60 GHz patch antenna a 1.85 mm (V) connector is utilized. There are many different vendors and option types to choose from but a suggested model is detailed from Southwest Microwave. The connector must be compatible with the dimensions of the designed patch antennas, taking into account considerations such as the height of the dielectric and the acceptable pins, which are separate components from the connectors themselves. Model number *1812-04SF* is ideal for the design described in this thesis. Figure 7.4 shows the specs of this connector.
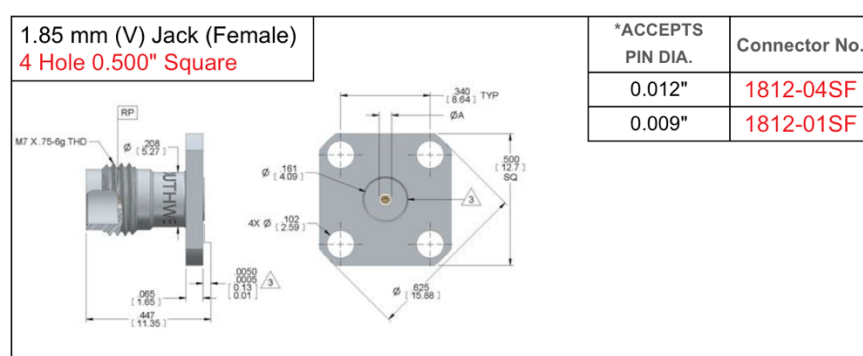
Figure 7.4: 1.85 mm SMA Connector

The 0.012" pin is needed because the associated launch pins satisfy the design constraints of the antenna design. Pin model *1090-05G* is a direct transition to stripline which can be utilized as the through put pin. The height of the pin is 0.025" which corresponds to 0.635 mm which can reach from the ground plane to the patch as the chosen dielectric is .508 mm thick. The pin specifications are shown in figure 7.5.

d Dia.: 0.012"
L: 0.050"
T: 0.025"

For Flange Mount Connectors

Launch Pin/Tab Transition to Stripline
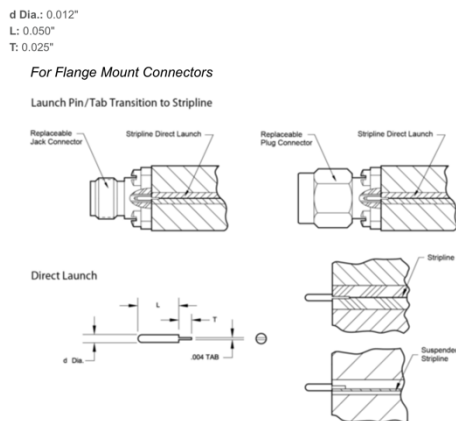
Figure 7.5: Launch Pin Specifications

Note that the length of the pin may need to be sanded down to create a flush connection with the antenna. Although this is not ideal, it is the best option with the resources available. To connect the SMA a screw and or a conductive glue can be utilized to attach the connector the ground plane of the patch. Once constructed, the antenna can then be tested and analyzed with a VNA.

7.3 Conclusion

This chapter described in detail the process of transferring the antenna design from CST to ADS and then exporting the necessary Gerber files for fabrication. From here the design would be sent to a fabrication house with the associated specification notes about the various components of the antenna. The connectors and launch pin accessories are also discussed in this chapter and can be ordered through Southwest Microwave vendors.

Chapter 8

Chapter 8 Conclusion

8.1 Thesis Summary and Conclusion

In this thesis, an investigation of rectangular microstrip patch antennas for operation 60 GHz was discussed. The applications and implications of this technology is far reaching, from revolutionizing next generation wireless communication to expanding on wearable device capabilities. Remote vital sign detection in particular is a use case that was discussed in great depth. 60 GHz patch antennas would provide greater accuracy for VSD and have a number of applications ranging from gaming to life saving devices. Techniques and details for creating different patch antennas were discussed and a 60 GHz 2x2 patch antenna array was designed. A design from the conducted literature survey was recreated and analyzed further and compared to a theoretical design of the 2x2 patch antenna. A solid cavity casing was then applied to improve front to back lobe ratio. The different backing dimensions had a major effect on the return loss and radiation pattern of the antenna, indicating that the cavity could be designed to optimize antenna performance. The patch design process was then repeated on a new dielectric material, R04350. Microstrip transmission line feed for a single patch and then a 2x2 patch array were designed. Cavity backing was implemented for the patch array and it was again observed that this has a major influence on the operational characteristics of the antenna. Due to the large foot print of the microstrip feed network and unwanted radiations, the antenna array radiation pattern was deteriorated. The feed transmission lines varied from high to low to high impedances causing undesired discontinuities, losses and excitation of unwanted surface waves. To get around this, a probe fed design was created for both single patch and patch array. The quarter wave transmission lines for the patch array were also redesigned to create a more gradual, high to low impedance transition from input to patch and reduce the occurrence of abrupt discontinuities. A via fence cavity was then designed for both single patch and 2x2 patch array. Using Via fence wall is the most realistic and applicable technique for creating a cavity in PCB fabrication process. Previous design guidelines from surveyed research did not hold and the parameters for the cavity needed to be determined by optimized parametric simulations. According to [11] the ratio of via cavity dimensions to patch dimensions should be twice the patch dimensions (R = 2a), and optimized at 1.8 times the patch for rectangular patch to rectangular cavity at 2.4 GHz. Through parametric sweeps at 60 GHz it was found that a via cavity backing ratio of 1.32 times the width of the patch and 2.59 times the length of the patch was optimal. For the 2x2 patch array it was determined that the cavity cross-sectional area should be 2.24 x antenna width by 2.42 x antenna length. From the multitude of sweeps it appeared that the width of the cavity had more of an influence on the general shape of the S11 curve while the length tinkered with the matching and S11 value. The cavities successfully improved the FTBLR of both single patch antenna and 2x2 patch antenna array, increasing the single patch gain by 1.75 dB and the array gain by 1.24 dB.

The process for fabricating and ordering necessary connectors to eventually test the antenna was also elaborated in this thesis.

8.2 Future Work Recommendations

In this thesis, finalized design and fabrication steps for 60 GHz microstrip patch antennas are created but the actual manufacturing and physical testing remain for future work. In addition, the peculiar results of the location of the probe feed should also be investigated. According to the parametric sweeps, the best location for the probe feed or inset microstrip feed was right on the edge of the patch which does differ from theoretical results. From fullwave simulation results, however, the edge of the patch matched the 50 Ω input better than any other location on the patch. There are a multitude of different applications for 60 GHz antennas, including wireless narrow band communication and remote VSD. Further investigation and testing could also be done with a specific use case in mind.

Bibliography

[1] Jones, Dan. "60GHz: A Frequency to Watch." *Light Reading*, 2014, www.lightreading.com/mobile/backhaul/60ghz-a-frequency-to-watch/d/d-id/709910.

[2] Bevelacqua, Pete. "Microstrip (Patch) Antennas." *Microstrip Antennas: The Patch Antenna*, 2011, www.antenna-theory.com/antennas/patches/antenna.php.

[3] Gulla, Sreedhar Kumar. "Circularly Polarized Circular Patch Antenna with Coplanar Parasitic Elements." *Research Gate*, 2016, www.researchgate.net/figure/302909421_fig3_Figure-4-Probe-fed-Rectangular-Microstrip-Patch-Antenna.

[4] Khaleel, Aymen Dheyaa. "Design Tri-Band Single and Dual Patch Array Antenna with Band Suppression." *Research Gate*, 2012, www.researchgate.net/figure/276353525_fig5_Figure-25-Microstrip-line-feed-with-rectangular-patch-antenna.

[5] Jean-Charles, Yves-Thierry, et al. "Effects of Substrate Permittivity on Planar Inverted-F Antenna Performances." *Journal of Computers*, vol. 4, no. 7, Jan. 2009

[6] Woo, Hyounggwan. "Discharge Observation on Antenna Surface Radiating High-Power Microwave in Simulated Environment." Research Gate, 2014, www.researchgate.net/figure/273244385_fig1_Fig-2-Nature-of-electric-field-when-a-patch-antenna-radiates-microwaves.

[7] "4G Ready Antenna Training Lab ATS04 | Amitec." *Amitec,* training.amitec.co/home/antenna-positioner-transmission-line/antenna-training-lab-ats04.

[8] Pellegrini, A., et al. "Antennas and Propagation for Body-Centric Wireless Communications at Millimeter-Wave Frequencies: A Review [Wireless Corner] - IEEE Journals & Magazine." *Design and Implementation of Autonomous Vehicle Valet Parking System - IEEE Conference Publication*, Wiley-IEEE Press, 2013, ieeexplore.ieee.org/document/6645205/.

[9] N. K. Vishwakarma, R. Samminga, A. Kedar and A. K. Singh, "Design considerations for a wide scan cavity backed patch antenna for active phased array radar," *2011 Indian Antenna Week (IAW)*, Kolkata, 2011, pp. 1-4.

[10] P. K. Singhal and S. Banerjee, "A cavity backed rectangular patch antenna," *6th International SYmposium on Antennas, Propagation and EM Theory, 2003. Proceedings. 2003*, Beijing, China, 2003, pp. 112-115.

[11] M. H. Awida and A. E. Fathy, "Design guidelines of substrate-integrated cavity backed patch antennas," in *IET Microwaves, Antennas & Propagation*, vol. 6, no. 2, pp. 151-157, January 31 2012.

[12] Bevelacqua, Pete. "Microstrip Antenna - Feeding Methods." *Antenna-Theory.com - Rectangular Microstrip (Patch) Antenna - Feeding Methods*, www.antenna-theory.com/antennas/patches/patch3.php

[13] C. Gu, C. Li, J. Lin, J. Long, J. Huangfu and L. Ran, "Instrument-Based Noncontact Doppler Radar Vital Sign Detection System Using Heterodyne Digital Quadrature Demodulation Architecture," in *IEEE Transactions on Instrumentation and Measurement*, vol. 59, no. 6, pp. 1580-1588, June 2010.

[14] H. C. Kuo and H. R. Chuang, "Investigation of carrier frequency effect on detection performance of Doppler sensor systems for noncontact human vital-signs sensing," *2014 8th International Symposium on Medical Information and Communication Technology (ISMICT)*, Firenze, 2014, pp. 1-4.

[15] Lin, Jenshan. *Microwave Doppler Radar Sensor for Detection of Human Vital Signs and Mechanical Vibrations*. *Microwave Doppler Radar Sensor for Detection of Human Vital Signs and Mechanical Vibrations*.

[16] C. Li, J. Cummings, J. Lam, E. Graves and W. Wu, "Radar remote monitoring of vital signs," in *IEEE Microwave Magazine*, vol. 10, no. 1, pp. 47-56, February 2009.

[17] J. C. Lin, "Noninvasive Microwave Measurement of Respiration," Proceedings of the IEEE, vol. 63, no. 10, p. 1530, Oct. 1975.
K.-M. Chen and H.-R. Chuang, "Measurement of Heart and Breathing Signals of Human Subjects Through Barriers with Microwave Life-Detection Systems," IEEE EMBC 1988.

[18] H.-R. Chuang, Y.-F. Chen, and K.-M. Chen, "Automatic Clutter Canceler for Microwave Life-Detection System," IEEE Trans. Instrumentation and Measurement, Vol. 40, No. 4, August 1991.

[19] C. Li, J. Lin, Y. Xiao, "Robust Overnight Monitoring of Human Vital Signs by a Non-contact Respiration and Heartbeat Detector," Proceedings of the 28th IEEE Engineering in Medicine and Biology Society Annual International Conference, pp. 2235-2238, September 2006

[20] Rappaport, Theodore S. "Introduction to Millimeter Wave Wireless Communications." *InformIT*, Pearson, Oct. 2014, www.informit.com/articles/article.aspx?p=2249780.

[21] Drew. "Wireless Nerd." *The Importance of Location in Wi-Fi. Wireless Field Day 8 at Cisco, Zebra, Aruba, and Levi's Stadium!*, 5 Oct. 2015, www.wirelessnerd.net/2015/10/the-importance-of-location-in-wi-fi.html.

[22] "Standard Gain Horn." *Shwarzbeck*, www.schwarzbeck.de/en/antennas/broadband-horn-antennas/standard-gain-horns.html.

[23] Wiltse, James C. "History of Millimeter and Submillimeter Waves - IEEE Journals & Magazine." *Design and Implementation of Autonomous Vehicle Valet Parking System - IEEE Conference Publication*, Wiley-IEEE Press, ieeexplore.ieee.org/stamp/stamp.jsp?tp=&arnumber=1132823.

[24] Peixeiro, Custodio. "Microstrip Patch Antennas: An Historical Perspective of the Development - IEEE Conference Publication." *Design and Implementation of Autonomous Vehicle Valet Parking System - IEEE Conference Publication*, Wiley-IEEE Press, 2012, ieeexplore.ieee.org/document/6169224/.

[25] *915MHz Patch Antenna - Saturn PCB Design*, www.saturnpcb.com/pa915.htm.

[26] Patel, Pragati. "What Is the Difference between AWR, HFSS, ADS, CST?" *Research Gate*, www.researchgate.net/post/What_is_the_difference_between_AWR_HFSS_ADS_CST.

[27] Hassan, Mohamed. *Design and Analysis of Substrate-Integrated Cavity-Backed Antenna Arrays for Ku-Band Applications*. University of Tennessee, 2011, trace.tennessee.edu/cgi/viewcontent.cgi?article=2119&context=utk_graddiss.